REMARKS

In response to the Office Action, claims 1-5, 7, 10, 12-14, and 16 have been amended to correct informalities in the claims.

Information Disclosure Statement

Applicant notes that the Office considered all of the references submitted in the Information Disclosure Statement received on March 6, 2006, except for "Air Traffic Control". Please note that the listing of this article in the Information Disclosure Statement was in error. The article entitled "Navigation, Sagnac Effect and Michelson Experiment" by M. Böhm identified in the IDS included a page with an advertisement by AEG Telefunken, which mentions "Air Traffic Control". Applicant's attorney inadvertently submitted this portion of the article by Böhm as a separate article when in fact it comprises part of the article by Böhm and should be considered as such by the Office. Applicant's attorney requests the Office to contact him if there is any question concerning this matter.

Objections to the Specification and Drawings[1]

At page 2 of the Office Action, the specification and drawings are objected to for failing to comply with the first paragraph of 35 U.S.C. 112. Applicant respectfully disagrees.

It is asserted by the Office that the description in the specification at page 7, line 32-page 8, line 8, is unrelated to the Sagnac effect, and that element 14 is disclosed as a device for measuring rotation, which is described exemplarily as a laser gyroscope. Further, the Office asserts Figure 1 could potentially have been used to describe Sagnac geometry for measuring rotation, but element 14 appears to be used for removing any rotational effects from the rest of Figure 1.

Figure 1 presents an embodiment of a device that can be used to determine its own translatory speed based on a detected change of phase in the emission parts leaving paths 11 and 12 at phase comparator 13. For the

measurement of this speed, rotational effects on a change of phase are to be compensated for in this embodiment to avoid any falsification of the speed measurement. Element 14 of the device of Figure 1 is included to provide data for such a compensation. This is also clear from the wording of claim 1, where it is stated "wherein the system is designed in such a way that a change in the phase displacement of the emission parts detected by the evaluation means for respectively one of the devices due to a rotational movement of this device is prevented or compensated for."

The Office further asserts that the configuration set forth in this paragraph does not comply with known physical laws and will not give a periodic interference signal based upon linear translations, as the speed of light is a constant as it moves across the two homogenous media (11 and 12) which are traveling in the same direction. Applicant respectfully disagrees. The specification clearly states that the paths 11 and 12 are "arranged in such a way that emission parts require different times to cover the route formed by the respective path" (Application as filed, page 7, lines 10-12). For example, the two paths can "be two optical fibers of equal length made of different materials with different refractive indices" (Application as filed, page 7, lines 14-16). The specification then proceeds to explain how these two paths specifically relate to giving a periodic interference signal, from page 7, line 32-page 8, line 8. Thus, Applicant respectfully disagrees that no interference signal is provided in the first embodiment cited by the Office.

Applicant also respectfully disagrees with the assertion that similar to the first embodiment, "embodiments two, three, and four are physically incapable of providing the listed functions as set forth in the specification, i.e. the four embodiments are physically incapable of measuring linear speed as set forth in the specification and drawings." With respect to the second embodiment described in the specification (see Figure 9 and page 9, line 6-page 10, line 13), it is clearly stated that

---

[1] The technical analysis set forth herein is based upon the analysis provided to applicant's attorney

> "[i]f the device is in a state of rest, then, because of the different route lengths, a specific phase displacement occurs between the emission parts. If the device moves with a direction component, which corresponds to the connection line between the emission location and the measuring location, then this phase displacement changes. The phase comparator 23 determines the amount of the change and, on the basis of this, the translatory speed of the device. (Application as filed, page 10, lines 4-8).

Thus, the specification clearly sets forth the manner in which this embodiment can measure linear speed. Similar disclosures are made with respect to embodiments three and four in the application as filed at page 10, lines 25-29 and page 12, lines 11-26, respectively. Therefore, Applicant respectfully submits that each embodiment disclosed in the specification is capable of measuring linear speed as set forth in the specification and drawings.

The Office also asserts that in the system of claim 1, by reciting at least six devices arranged in different spatial directions, the Applicant is referring to fourth, fifth and sixth dimensions. Applicant submits that the Office has misunderstood the use of six devices measuring the speed in a respective direction. It is by no means assumed or suggested by Applicant that there is a fourth, fifth or sixth dimension of space in the present application. Claim 1 requires that the six devices are arranged in different spatial directions, not along different dimensions. An arrow in a three-dimensional space can obviously point in infinite spatial directions, not only in three directions. For example, six different directions in a Cartesian coordinate system could be the x, -x, y, -y, z and -z directions.

The presented approach is provided for measuring translation and rotation of a system. With three measuring devices measuring their own speed, for example in directions x, y and z, respectively, it is only possible to measure the complete translation. But it is not possible to also measure the complete rotation.

Consider a single measuring device that is able to measure its speed in the direction of the arrow below:

This device is only able to measure a translatory movement from left to right and vice versa. Now consider a pair of measuring devices that are arranged, e.g. on two opposite sides of a cube, as indicated by arrows below:

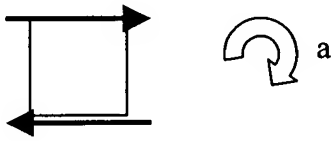

When the cube rotates as indicated by the arrow a, the upper device by itself will only detect a translatory movement from left to right. The lower device by itself will only detect a translatory movement from right to left. But if the measurement results of both devices are considered together, it is clear that whenever the upper device indicates a movement to the right while the lower device indicates at the same time a movement to the left, the cube has to undergo a rotational movement.

The same logic applies to the other two "dimensions." Thus, for determining all components of speed and rotation of a system, six speed-measuring devices are required. Therefore, Applicant respectfully disagrees with the Office's assertion that "the specification's and claims' reliance on the fourth, fifth, and sixth device for completely describing the speed of the system is nonsensical."

At page 2, the Office asserts the following: "[t]he Sagnac effect is not a phenomenon of linear displacement, but rather rotational displacement, and it is measured by utilization of a closed-loop geometry. What the applicant is describing in [the paragraph spanning from page 7, line 32-page 8, line 8 of the specification] appears to be unrelated to the Sagnac effect." Any subsequent argumentation of the Office is then based on this interpretation of physical laws. The Office does not provide any explanation how the described invention is to be

interpreted instead, and due to which effects the presented differences result. Thus, Applicant submits that this statement is only an unfounded and unsubstantiated rejection.

In order to explain the basics of the invention, an experiment is cited that is based in the U.S.A. and which is repeated each and every day millions of times: The Global Positioning System (GPS). GPS uses a triangulation, which is based on the finiteness of the speed of light. A receiver requires data on position and time from at least four satellites in order to be able to determine its own position. The accuracy of the positioning depends not only on these data, but also on the physical surrounding conditions. The known and measurable influences, which result in a deviation of the ideal triangulation, are divided into three classes. The division into three classes results in principle from the order of magnitude, which is the quantifiable value, of the deviation.

First, there are effects that are caused by the atmosphere of earth. Due to refraction of electromagnetic waves and diffraction, these effects result in a change of the ideal transmission path of the waves. Thus, the location of the transmitter– from the point of view of the receiver - is not the location that is indicated by the signal. These deviations depend on the weather in the region of the receiver and the position of the transmitter (GPS satellite) over the horizon.

Second, there are the relativistic errors, which result from the movement of the transmitter and the gravitational field of Earth. Both time dilatations add to a total dilatation and are compensated by offsetting a clock in the GPS satellites.

Third, there is the Sagnac effect, which is caused by the rotation of earth, and which means a further deviation in the computations of the location in dependency of the latitude. The Sagnac effect is of great importance, for example, in the precise positioning of precision bombs of the U.S. military, where millimeters are of importance, but is of no importance for other navigation purposes, since the effect is too small.

The Sagnac effect is based in this context on the velocity with which the receiver moves on the surface of the Earth – on the one hand moving itself and

on the other hand moved by the rotation of earth. In this constellation, however, there is no "closed-loop geometry", which is considered by the examiner to be a precondition for the Sagnac effect. In the present invention, a linear, open configuration as described in the patent application and the patent claims is given.

Thus, it has to be asserted that the U.S. military is well informed about a Sagnac effect that occurs in linear and open situations; it is able to measure this effect and to use this effect in the control of its military means. Furthermore, scientists of various countries know this effect and take it into account in their calculations. This can be taken from many publications.

By way of example, a copy of a publication from Syracuse University is attached (Attachment A).[2] This document states "[t]here is also effect (Sagnac delay) caused by the Earth's rotation during the time of transit of the satellite signal from satellite to the ground." It is also stated, that "[i]f we use inertial frame of reference, clocks could be synchronized using Einstein's synchronization procedures. ... However users of GPS are moving (Earth is rotation) and noninertial effect take place. ... Sagnac effect plays important role in the system. ..."

As a further example, a copy of the following Web-site is attached, which equally mentions the relevance of the Sagnac effect for GPS: http://www.kowoma.de/en/gps/errors.htm (Attachment B). It states: "There is another relativistic effect, which is not considered for normal position determinations by GPS. It is called Sagnac-Effect and is caused by the movement of the observer on the earth surface, who also moves with a velocity of up to 500 m/s (at the equator) due to the rotation of the globe. The influence

[2] This document is also available at http://physics.syr.edu/courses/PHY312.03Spring/GPS/GPS.html. It is further respectfully submitted that this document and the additional documents identified below (Attachments B and C) are technical background documents that do not require submission in an IDS. If the Office considers otherwise, applicant will submit same in an IDS.

of this effect is very small and complicate to calculate as it depends on the directions of the movement. Therefore it is only considered in special cases."

Consequently, the above assumption forming the principal basis of the rejection of the examiner is not maintainable, as it is clear that the Sagnac effect is not limited to a closed-loop geometry.

Furthermore, the Office is kindly requested to consider the following experiment and the question resulting from it, which has not been answered so far, as can be taken as well from generally accessible literature:

The experiment relates again to GPS and the related and measurable deviations from the ideal triangulation, in particular the Sagnac effect which can be measured, and of which it has been shown above that it is based on a linear change (prolongation or shortening) of the path due to the proper motion of objects.

The velocity of the rotation of Earth at the equator is approximately 500 m/s. The velocity of the Earth revolving around the Sun is on average approximately 29,783 m/s, thus approximately 60-fold. Moreover, consider for reasons of simplicity, only the projection of all movements of the GPS satellites onto the plane of the orbit of the Earth around the Sun. The experimenter is a stationary observer looking from above onto this system (Sun - Earth - GPS satellites). Of all possible constellations of these objects that can be observed, at first mainly those in which GPS satellite and Earth revolve in the same direction around the Sun are considered.

When considering only Earth and GPS satellite, as already described above, it is known there is the Sagnac effect due to the rotation of earth, i.e. the deviation based on the moving away of the receiver from the location at which it was when the signal was transmitted by the GPS satellite. It is also known that the deviation can be measured and how large it is.

However, if the experimenter is located outside of the solar system and can see the whole picture, the following can be observed: Since Earth, and thus the receiver, are moving with the 60-fold velocity in addition from the location at

which it was when the signal was transmitted by the GPS satellite, and since the Sagnac effect is obviously existent, the experimenter would have to consider in addition this movement, and expect a deviation induced by the Sagnac effect which is 60-fold larger than the one which is actually observed. But this is not the case. The experimenter would only see the Sagnac effect that is induced by the rotation of Earth.

The consequence of this is that an observer from outside the system would see in this constellation of objects a real signal (which is obviously confirmed millions of times a day) propagating faster than with the speed of light from the location at which it was transmitted to the location at which it reaches the receiver. This is a real experiment installed by the U.S.A., which shows that an attitude of considering the theories of relativity of Mr. Einstein as unalterable is not justified.

An explanation is given by Mr. Fizeau, certainly not unknown to Mr. Einstein, whose experiments about 50 years before Einstein only have to be considered in a new light. For the comprehension of the effect according to Fizeau a further source is cited with a recently published experiment: "Transverse Fresnel-Fizeau drag effects in strongly dispersive media" by I. Carusotto, M. Artoni, G.C. La Rocca and F. Bassani, published on June 9, 2003 with PACS numbers 42.50.GY and 42.25.Bs, a copy of which is attached hereto (Attachment C). This experiment shows a completely different understanding of the observations of Fizeau, who still assumed a change of the index of refraction. In the meantime, however, it is possible to show the coupling of light to material outside of conditions of reflection, which means that light does not propagate inertially, as assumed until now. Therefore, the theories of Mr. Einstein cannot and are not considered to be valid universally anymore.

Lastly, the Office appears to assert that by invoking "Doppler" at page 13 of the specification, the Applicant is also disclosing that the invention requires a "luminferous aether." Applicant cannot find any direct relationship between these two concepts that would lead to a conclusion that the invention requires light to

travel in a luminiferous aether. The application as filed makes no mention of the luminiferous aether, nor does it suggest that it is required for the invention to be operable. The application as filed mentions in several instances that the at least one path of claim 1 can be an optical fiber, but there is no discussion relating to luminiferous aether (*See, e.g.,* Application as filed, page 3, line 25; page 4, lines 24-26; page 5, lines 24-25; page 7, lines 14-16; page 11, lines 12-17). The Office has also failed to explain the connection between Applicant's mention of Doppler and an inherent requirement that a luminiferous aether is required by the invention. Therefore, Applicant respectfully disagrees with the Office's assertion that the current invention requires light to travel in a luminiferous aether and is therefore inconsistent with modern physics.

For all of the foregoing reasons, Applicant respectfully submits that the Office's objections to the specification and drawings as failing to comply with the first paragraph of 35 U.S.C. 112 should be withdrawn, and the specification and the drawings are in allowable form.

Claim Rejections- 35 U.S.C. 101

At page 5 of the Office Action, claims 1-18 are rejected under 35 U.S.C. 101 because it is asserted the disclosed invention is inoperative and therefore lacks utility. Applicant respectfully disagrees.

The Office rejects the claims under §101 because it is asserted the invention is inoperative because it "measures linear translations of self-contained devices based on the theory that the luminiferous aether exists." As stated above, there is nothing disclosed in the application as filed which suggests the invention is based on the theory that the luminiferous aether exists. Therefore, for all of the reasons stated above with respect to the objections to the specification and drawings, it is respectfully submitted that the invention disclosed in claims 1-18 is operative and are allowable under §101.

Claim Rejections- 35 U.S.C. 112

At page 6 of the Office Action, claims 1-18 are rejected under 35 U.S.C. 112, first paragraph, as failing to comply with the enablement requirement. It is asserted that the claims contain subject matter which was not described in the specification in such a way as to enable one skilled in the art to which it pertains, or with which it is most nearly connected, to make and/or use the invention. Specifically, the Office has asserted that the disclosure fails to describe devices capable of providing the claimed function of measuring speed. As Applicant has argued above in reference to the objections to the specification and drawings, the application as filed fully describes how the claimed system and devices are capable of measuring speed and rotation. Therefore, it is respectfully submitted that the current invention set forth in the claims is sufficiently enabled and operable, such that proof of actual reduction to practice should not be required at this time.

Furthermore, the Office rejects claims 1 and 10 under 35 U.S.C. 112, second paragraph for indefiniteness. Applicant has amended these claims in a manner so as to correct the indefiniteness asserted by the Office. Therefore, it is respectfully submitted that the claims are in allowable form under 35 U.S.C. 112.

In view of the foregoing, it is respectfully submitted that the present application as amended is in condition for allowance and such action is earnestly solicited.

The undersigned respectfully submits that no fee is due for filing this Amendment. The Commissioner is hereby authorized to charge to deposit account 23-0442 any fee deficiency required to submit this paper.

Respectfully submitted,

Dated: October 21, 2009

Alfred A. Fressola
Attorney for Applicant
Reg. No. 27,550

WARE, FRESSOLA, VAN DER SLUYS
& ADOLPHSON LLP
Bradford Green, Building Five
755 Main Street, P.O. Box 224
Monroe, CT 06468
Telephone: (203) 261-1234
Facsimile: (203) 261-5676
USPTO Customer No. 004955

Global Positioning System

Some Graphics Below have been borrowed from the references

PHY 312

5/6/98

The Global Positioning System (GPS), which was developed to meet military needs of the Department of Defense but now is used in every day life, is a radio based navigation system that gives three dimensional coverage of Earth 24 hours a day in any weather condition. It is the only system today able to show your exact position on the Earth anytime, anywhere and it is one of history's most exciting and revolutionary developments. The GPS system can tell location anywhere on or above the Earth within about 300 feet. Greater accuracy could be achieved (within less then three feet) with corrections calculated by a GPS receiver at a known fixed location. The Department of Defense developed and maintains GPS. Even though the system has been completed only recently it has already proved to be a most valuable aid to U.S. military forces. Operation Desert Storm was performed using GPS. Soldiers were able to go places and maneuver in sandstorms or at night even when he troops who lived there couldn't. Navy ships use GPS for rendezvous, minesweeping, and aircraft operation. GPS is also used for navigation in planes, ships, cars, and trucks. GPS has become important in almost all military operations and weapon systems.

GPS consists of three parts: the space segment, the control segment and user segment.

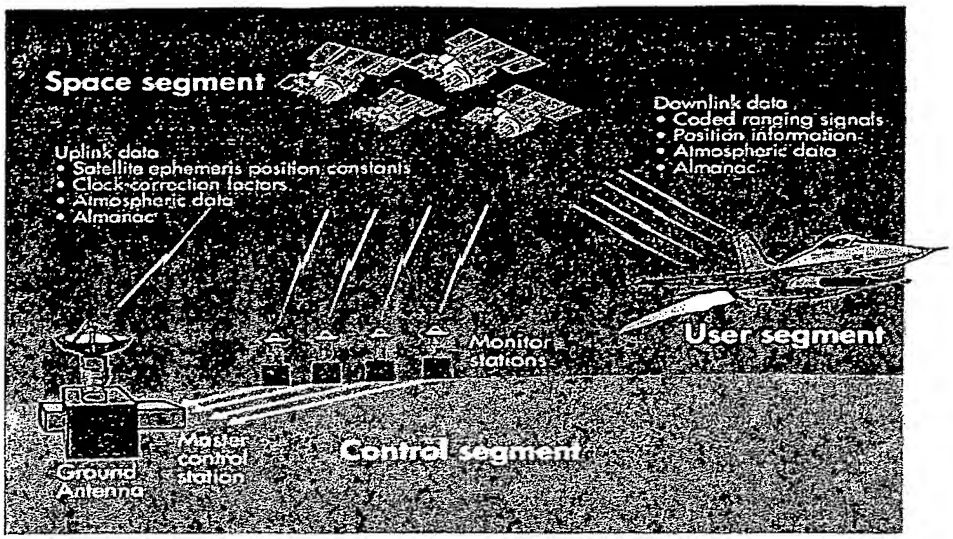

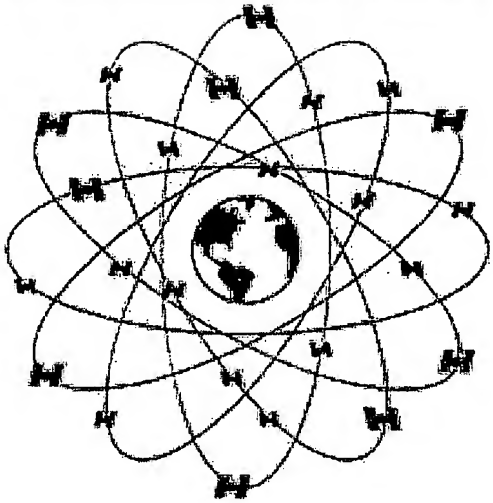

The space segment consists of satellites, 24 in all: 21 navigational SVs and 3 active spares orbit at 11,000 nautical miles above the Earth. There are six orbital planes (with 4 SVs in each), equal spaced (60 degrees apart), and inclined about 55 degrees with respect to the equatorial plane. This constellation provide the user with the ability to receive the signal form five to eight SVs nearly 100% of the time at any position on Earth. It takes12 hours each to go around the Earth once (one orbit). Clocks in satellites keep accurate time to within three nanoseconds - that's 0.000000003 of a second. "Clock-driven transmitters send out synchronous time signals, tagged with the position and time of the transmission event, so that a receivers near the Earth can determine its position and then by decoding navigation messages from four satellites to find the transmission event coordinates, and then solving four simultaneous one-way signal propagation equations" (Ashby, Neil). Conversely, gamma-ray detectors on the satellites could determine space-time coordinates of a nuclear event by measuring signal arrival times and solving four one-way propagation delay equations. The time is very important because the receiver must determine exactly how long it takes for signal to travel from each GPS satellite. Satellites transmit the signals that can be detected by anyone with GPS receiver. Satellites paths are monitored by ground stations. The first GPS satellite was launched in 1978 and first 10 satellites were developmental satellites, called Block I. From 1989 to 1993 23 additional production satellites, called Block II, were launched. The launch of 24^{th} satellite in 1994 completed the system.

The GPS control segment consists of a system of monitor stations located around the world (Hawaii and Kwajalein in the Pacific Ocean; Diego Garcia in the India Ocean; Ascension Island in the Atlantic Ocean; and Colorado Springs, Colorado) a master ground station at Falcon Air Force Base in Colorado Springs, Colorado; and four large ground antenna stations that broadcast signals to the satellites.

Global Positioning System (GPS) Master Control and Monitor Station Network

Monitor stations measure signal from SVs which are incorporated into orbital model of each satellites. The models compute orbital data and clock correction for each satellite. Master Control station uploads orbital and clock data to SVs which send subsets of the data to GPS receivers over radio signals.

GPS user segment consists of receivers which could be hand carried or installed on aircraft, ships, tanks, submarines, cars, and trucks. Receivers detect, decode, and process GPS satellite signals. The signal is converted into position, velocity, and time estimates. In total there are five pieces of data that GPS receiver can take measurements on. Receiver records positions in Latitude and Longitude which can be translated in various Datums and coordinate systems for mapping.

There are two GPS Positioning Services specified in the Federal Radionavigation Plan:

a. Precise Positioning Service (PPS)

Authorized users with specially equipped receivers use PPS. Accuracy:

22 meter horizontal accuracy

1. meter vertical accuracy

100 nanosecond time accuracy

a. Standard Positioning Service (SPS)

Most receivers are capable of receiving and using SPS signal. Accuracy:

100 meter Horizontal accuracy

156 meter Vertical accuracy

340 nanoseconds time accuracy

The principle behind GPS is the measurement of distance or "range" between receiver and the satellites. The satellites also tell us exactly where they are in their orbits above the Earth. The problem is that by measuring time, Doppler shifts, gravitational frequency shifts and propagation delays has to be taken into account so the user could determine position accurately. An error of a billionth of a second in time corresponds to an error in location of 1 foot.

GPS is one of the first operating systems, excluding high-energy accelerators, that has important effects from relativity. When the first satellite was launched in 1997 there was still a lot of controversy about the Einstein's theory of Special and General Relativity. First satellite contained the first Cesium clock to be

placed in the orbit and there was a lot of people who doubted that relativity effects are real. A frequency synthesizer was build into satellite clock system so that after launch, if it proved to be that clock would run at the rate predicted by the General Relativity, it could be turned on to bring clocks in the coordinate rate necessary for operation. The clock on board was operated for about 20 days without turning on the synthesizer and the frequency measure during that interval was 442.5 parts in 10^{12} faster then the clocks on the ground. If no correction would of took place this would resulted in error of about 38,000 nanoseconds per day. The frequency predicted by General Relativity was only within 3.97 parts of 10^{12} which was within accuracy capabilities of orbiting clock. It is not easy right now to perform relativity tests using GPS because satellite clocks are actively corrected to within 1 microsecond of Universal Coordinated Time.

There are several reasons that relativity is very important in GPS: GPS satellites have a large velocity, there is large gravitational potential differences between that of the satellites and that of the users, and there is significant Earth rotation effects. These effects themselves might not be that important but because GPS satellites are equipped with atomic clocks relativistic effect should be taken into account.

"There are three primary consequences of relativity effects:

1. There is a fixed frequency offset in the satellite's clock rate when observed from Earth. Most of the effect is purposely removed by slightly offsetting the satellite clocks in frequency prior to launch, the so-called "factory offset" of the clock.
2. The slight eccentricity of each satellite orbit causes an additional periodic clock error effect that varies with the satellite's position in its orbit plane.
3. There is also effect (Sagnac delay) caused by the Earth's rotation during the time of transit of the satellite signal from satellite to the ground" (Parkinson, Bradford. pg. 623-634).

Moving users on the Earth surface or near it or fixed users at some altitude about the Earth surface have to make additional corrections caused the their velocity and the height above the ground.

The net effect of relativity for a zero eccentricity GPS satellite is a combination of effects caused by satellites velocity (Special Relativity effect) and Earth gravitational field (General Relativity effect). This produces small fixed frequency offset in addition to classical Doppler shift.

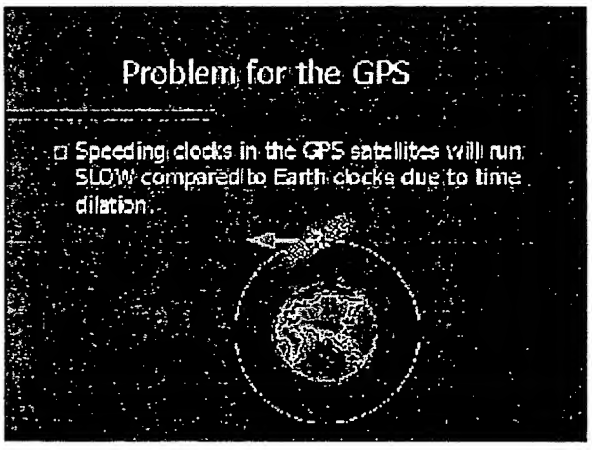

One of the effects of Einstein's Special Relativity theory is time dilation. Clocks moving with high velocity run slower then clocks with the smaller relative velocity. Therefore, clocks in the GPS satellites will run slower compare to the clocks on the Earth because GPS satellites have a large velocity. In more details the rates that clocks tick compare to the static clock are given by the formulas:

$Te^2 = (1 - Ve^2/c^2)Ts^2$; and $Tg^2 = (1 - Vg^2/c^2)Ts^2$, where Te is proper time of the clock on the surface of the Earth, Ve is the clock's linear velocity due to the rotation of Earth, Ts is proper time of static clock, Tg is proper time of the clock in the GPS satellite, Vg is linear velocity of the GPS satellite in the orbit. Therefor the ratio at which clock will tick could be derived from the formulas above: $Te^2/Tg^2 = (1 - Ve^2/c^2)/ (1 - Vg^2/c^2)$. This effect has a fixed value. Clocks in the GPS satellites run slow by 6 millionth of a second per day.

The effect of General Relativity is that clocks at the higher altitude above the Earth run faster then the clocks on the surface of the Earth. From the Schwarzschild metric we could calculate the rates at which clocks of particular interest tick compare to the clocks at infinite distance from source of gravitational field. Lets compare the rates of two static clocks: one on the surface of the Earth and other in the GPS

satellite. For a static clock:

$dT^2 = -dS^2 = (1 - R/r)dTi^2$, where T is proper time of the clock we interested in, Ti is proper time of the clock infinite distance away, and $R = 2MG/c^2$, where M is mass of the Earth, G is Newtonian gravitation constant and c is speed of light. Therefore the ratio of rates at which clock on the surface of Earth and in GPS satellite will tick is given by formula:

$dTe^2/dTg^2 = (1 - R/re)/(1 - R/rg)$, where re is radius of Earth and rg is distance from the center of the Earth to GPS satellite. This effect also has a fixed value. The clocks in the GPS satellites run fast by 45 millionth of second per day. Therefore combining Special and General Relativity effects we conclude that clock in GPS satellites run fast by 39 millionth of a second per day which if not taken into account could produce position error of 12 kilometers.

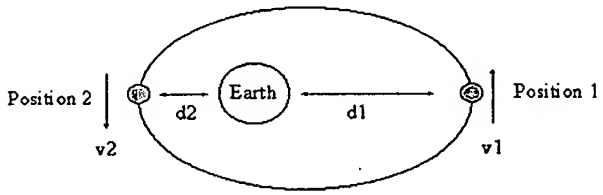

GPS satellites do not follow strict circular orbit around the Earth. There exist slight orbit eccentricity and therefore it causes periodic clock error effect that varies with satellites position in the orbit. Consider two positions of the satellite in the orbit (Position1 and Position2 in the diagram). As we could see, distance d1 from the Earth to the satellite in Position1 is not equal to distance d2 from the Earth to the satellite in Position2. Also there is differences in velocities at which satellite travels in those two positions. Velocity of satellite is Position2 will be bigger then velocity of satellite in Position1. Therefore there is going to be different Special and General relativity effect when satellite orbits around the Earth. GPS orbit around the Earth is very close to the circle, so periodic errors are very small but have a fixed values and could be included in the system.

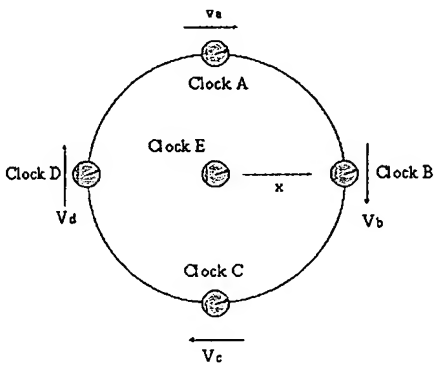

Simultaneity is very important concept in GPS. For users to determine position and time clock in the GPS satellites have to be synchronized. If we use inertial frame of reference, clocks could be synchronized using Einstein's synchronization procedures (if light rays emitted from two different points arrive at the midpoint of those points at the same time, then the events or transmitting the light ray from two original points occurred simultaneous). However users of GPS are moving (Earth is rotating) and noninertial effect take place. Consider situation illustrated in diagram above. Clocks A, B, C, and D are rotating around some fixed clock E. Velocities of the clocks are given by Va, Vb, Vc, Vd. Furthermore all velocities are equal and there exist centripetal (??) acceleration which causes clocks to move around clock E and therefore direction of velocities are changing with respect to coordinate axis x (represented in the diagram). Sagnac effect plays important role in the system. It would be desirable to synchronize clocks in the rotating frame fixed to the Earth because most of GPS users are at the rest or nearly so on the Earth's surface. Because Earth rotates, Sagnac effect is large enough in the GPS and the clocks can't be synchronized in the rotating frame and there is necessity for different approach to synchronize the clocks. Lets try to draw space-time diagram in the reference frame of clock E from diagram above. Lets choose a particular moment in time when velocity of clock A is in x direction, velocity of clock C is in direction opposite to x direction and velocities of clocks B and D in x direction is equal to zero. This situation is illustrated in the previous diagram. So space-time diagram looks like this:

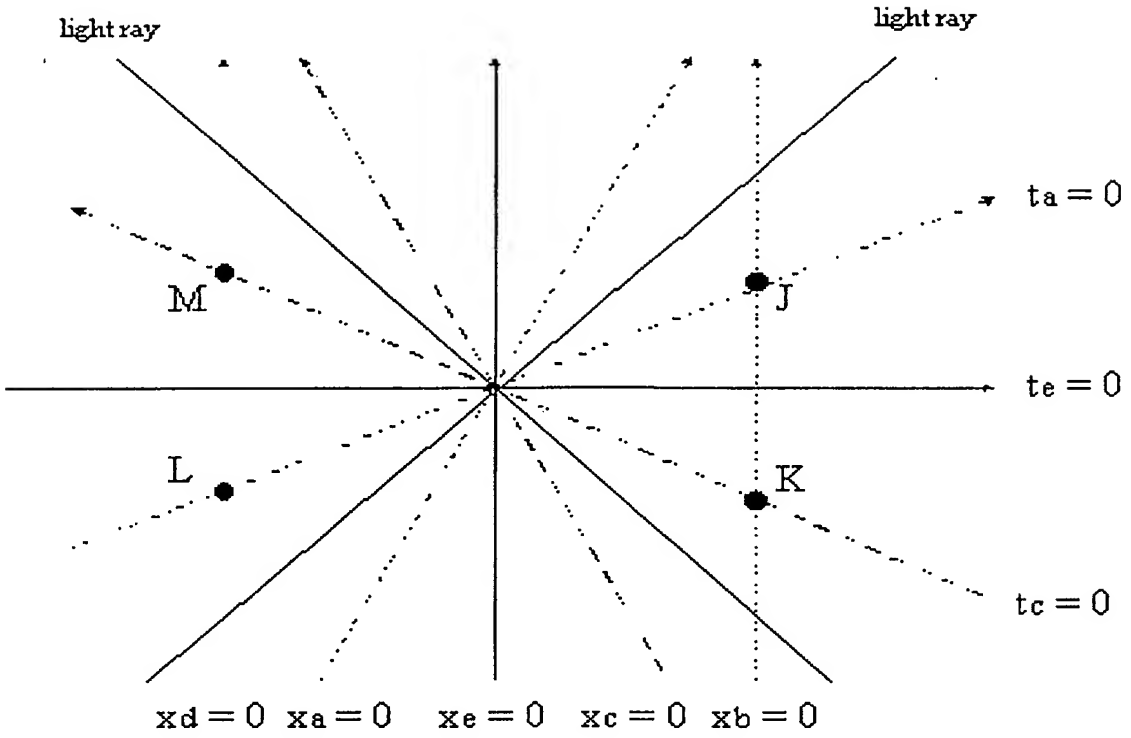

Notice that velocities of clocks D and B are zero so their world lines are parallel to the world line of cock E and lines of simultaneity are the same as for clock E. What does it meat for clocks A, B, C, and D to be synchronized? At any point in time all of these clock should show the same time coordinate. Say we use reference frame of clock A. Lets look at the diagram. Consider clocks A some line of simultaneity (ta = 0 in our diagram). Points J and L represent crossings with clock B and D world lines. If clocks are synchronized, clock B and D at the points J and L should read the same time as clock A (ta = 0). We could clearly see from the picture that when clock A reads time ta = 0, clock B reads time te>0 and clock D reads time te<0. Same analysis apply in the reference frame of the clock C (points M and K on world lines of clocks D and B). Therefore we can't synchronize clock using any rotating frame of reference. In the GPS synchronization is performed in the Earth-Centered Inertial frame using constancy of speed of light.

In addition to relativity effects explained above there exist effects caused by the user velocity and height of the user above geoid. Some of these effect might cancel or partially cancel in estimation of the position. However these effects might be significant if the user is another satellite in orbit.

There also exist secondary effects that are smaller then the accuracy level required by the user. Tidal potential effect on the clocks is result of the rotating Earth revolving around the Sun and therefore exposed to Sun's gravitational field. However, both the GPS satellites and the user are in orbit around the Sun at almost the same position so a lot of this effect cancels.

The Earth's gravity potential is not spherical because of the ellipsoidal shape of the Earth, which cause effect which is not modeled into the system (quadrupole field effect). However this effect is also very small. If higher accuracy is desirable for GPS system then this effect should be taken into account. If this effect is not taken into account gravitation potential of the Earth (F) is given by the formula:

F = -G*Me/r, where G is Newtonian gravitational constant, Me is the mass of the Earth, and r is distance from the observation point to the center of the Earth. This formula is consistent with spherical shape of the Earth. If we want to account for ellipsoidal shape of the Earth we extend our formula to account the factor $1/r^2$. Therefore,

$F = (GMe/r) * [1 - J_2(Re/r)^2 P_2(\cos Q)]$, where J_2 is Earth quadrupole moment coefficient, Re is the Earth's equatorial radius and $P_2(x) = (3x^2 - 1)/2$ is Legendre polynomial of second degree. This extension is sufficient for desirable accuracy of GPS but if military applications will require higher and higher accuracy from GPS system Gravitation Potential might need to be extended to account for Earth's not perfect ellipsoidal shape (this means that reciprocals of the higher powers of r will have to be included in the formula).

Another effect of the clocks in the GPS satellites is so called Shapiro delay. The cause of this delay is that light's velocity changes when it is exposed to Earth gravitational field. This delay was measured experimentally and was proved to be negligible.

Another effect on clocks is cause by Earth's mass rotating on its axis (Lense-Thirring effect - frame dragging). This effect slightly modifies solution to Einstein's equations and generates slightly different metric. However these effects are negligible for the purposes of GPS.

Relativistic effects in GPS system is very important. If higher accuracy will be desirable secondary effects of relativity will have to be implemented in the improved systems together with primary effects. Currently uncertainty of position using Precise Positioning Code is now around 2.4 meters and a lot of people are interested in reducing the error to the millimeter level. Even though the system is not at that high accuracy, it still provides a lot of examples for the applications in relativity.

"New and surprising applications of positioning determination and time transfer based on GPS are continually being invented. Civilain applications include for example, tracking elephants in Africa, studies of crustal plate movements, surveying, mapping, exploration, salvage in the open ocean, vehicle fleet tracking, search and rescue, power line fault location, and synchronization of telecommunications nodes" (Ashby, Neil).

Bibliography

Ashby, Neil. "General Relativity in the Global Positioning System".

http://vishnu.nirvana.phys.psu.edu/mog/mog9/node9.html

Dana, Peter. "Global Positioning System Overview".

http://www.utexas.edu/depts/grg/gcraft/notes/gps/gps.html

Ashby, Niel in "Global Positioning System: Theory and

Applications" by Parkinson, Bradford and Spilker, James.

2009-04-19

Sources of Errors in GPS

Selective Availability

The most relevant factor for the inaccuracy of the GPS system is no longer an issue. On May 2, 2000 5:05 am (MEZ) the so-called selective availability (SA) was turned off. Selective availability is an artificial falsification of the time in the L1 signal transmitted by the satellite. For civil GPS receivers that leads to a less accurate position determination (fluctuation of about 50 m during a few minutes). Additionally the ephemeris data are transmitted with lower accuracy, meaning that the transmitted satellite positions do not comply with the actual positions. In this way an inaccuracy of the position of 50 – 150 m can be achieved for several hours. While in times of selective availability the position determination with civil receivers had an accuracy of approximately 10 m, nowadays 20 m or even less is usual. Especially the determination of heights has improved considerably from the deactivation of SA (having been more or less useless before).

The reasons for SA were safety concerns. For example terrorists should not be provided with the possibility of locating important buildings with homemade remote control weapons. Paradoxically, during the first gulf war in 1990, SA had to be deactivated partially, as not enough military receivers were available for the American troops. 10000 civil receivers were acquired (Magellan and Trimble instruments), making a very precise orientation possible in a desert with no landmarks.

Meanwhile SA is permanently deactivated due to the broad distribution and world wide use of the GPS system.

The following two graphs show the improvement of position determination after deactivation of SA. The edge length of the diagrams is 200 m, the data were collected on May 1, 2000 and May 3, 2000 over a period of 24 h each. While with SA 95 % of all points are located within a radius of 45 m, without SA 95 % of all points are within a radius of 6.3 m.

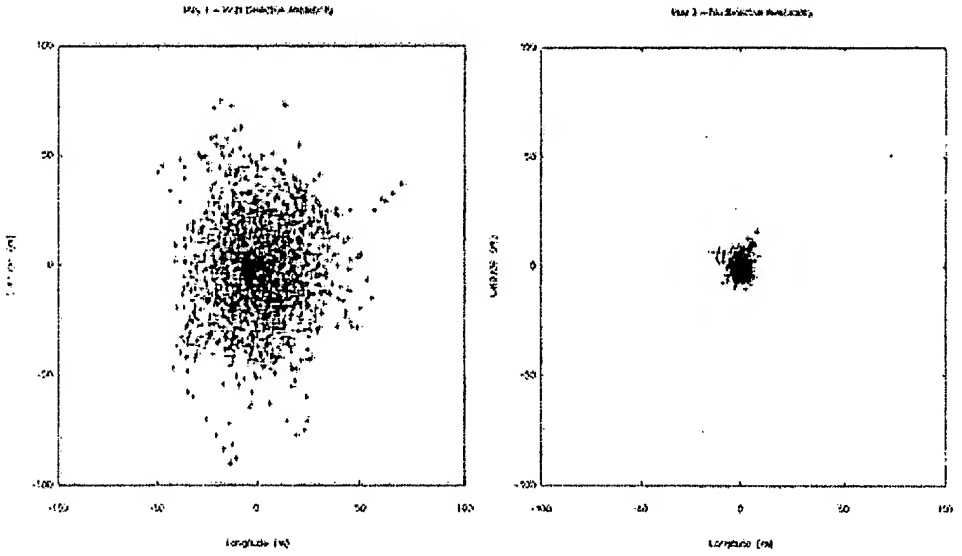

Plot of the position determination with and without SA
(Diagram from http://www.igeb.gov/sa/diagram.shtml (page no longer available)
With friendly permission of Dr. Milbert (NOAA))

"Satellite geometry"

Another factor influencing the accuracy of the position determination is the "satellite geometry". Simplified, satellite geometry describes the position of the satellites to each other from the view of the receiver.

If a receiver sees 4 satellites and all are arranged for example in the north-west, this leads to a "bad" geometry. In the worst case, no position determination is possible at all, when all distance determinations point to the same direction. Even if a position is determined, the error of the positions may be up to 100 – 150 m. If, on the other hand, the 4 satellites are well distributed over the whole firmament the determined position will be much more accurate. Let's assume the satellites are positioned in the north, east, south and west in 90° steps. Distances can then be measured in four different directions, reflecting a „good" satellite geometry.

The following graph shows this for the two-dimensional case.

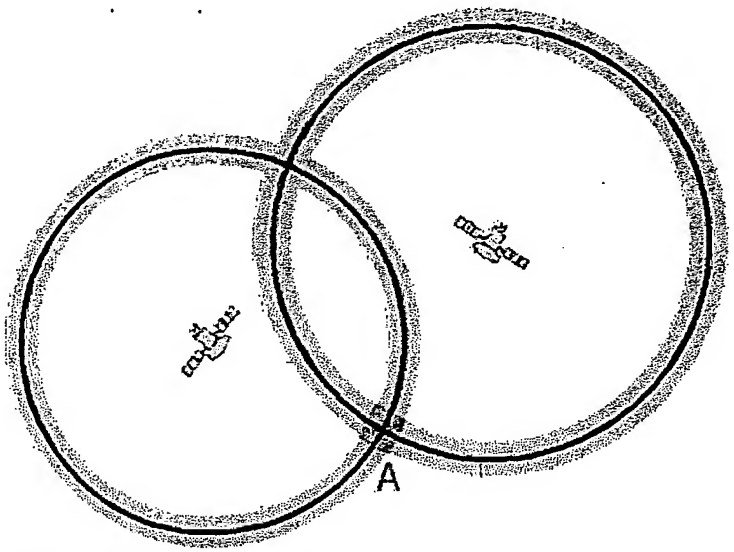

Good geometrical alignment of two satellites

If the two satellites are in an advantageous position, from the view of the receiver they can be seen in an angle of approximately 90° to each other. The signal runtime can not be determined absolutely precise as explained earlier. The possible positions are therefore marked by the grey circles. The point of intersection A of the two circles is a rather small, more or less quadratic field (blue), the determined position will be rather accurate.

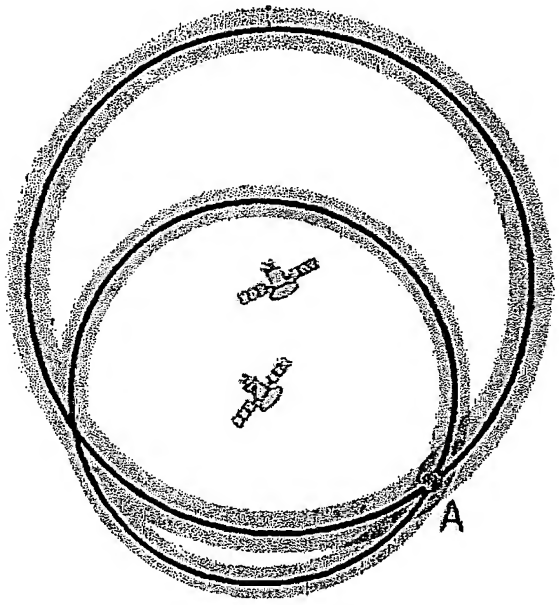

Bad geometrical alignment of two satellites

If the satellites are more or less positioned in one line from the view of the receiver, the plane of intersection of possible positions is considerably larger and elongated- The determination of the position is less accurate.

The satellite geometry is also relevant when the receiver is used in vehicles or close to high buildings. If some of the signals are blocked off, the remaining satellites determine the quality of the position determination and if a position fix is possible at all. This can be observed in buildings close to the windows. If a position determination is possible, mostly it is not very accurate. The larger the obscured part of the sky, the more difficult the position determination gets.

Most GPS receivers do not only indicate the number of received satellites, but also their position on the firmament. This enables the user to judge, if a relevant satellite is obscured by an obstacle and if changing the position for a couple of meters might improve the accuracy. Many instruments provide a statement of the accuracy of the measured values, mostly based on a combination of different factors (which manufacturer do not willingly reveal).

To indicate the quality of the satellite geometry, the DOP values (dilution of precision) are commonly used. Based on which factors are used for the calculation of the DOP values, different variants are distinguished:

- GDOP (Geometric Dilution Of Precision); Overall-accuracy; 3D-coordinates and time
- PDOP (Positional Dilution Of Precision) ; Position accuracy; 3D-coordinates
- HDOP (Horizontal Dilution Of Precision); horizontal accuracy; 2D-coordinates
- VDOP (Vertical Dilution Of Precision); vertical accuracy; height
- TDOP (Time Dilution Of Precision); time accuracy; time

HDOP-values below 4 are good, above 8 bad. HDOP values become worse if the received satellites are high on the firmament. VDOP values on the other hand become worse the closer the satellites are to the horizon and PDOP values are best if one satellite is positions vertically above and three are evenly distributed close to the horizon. For an accurate position determination, the GDOP value should not be smaller than 5. The PDOP, HDOP and VDOP values are part of the NMEA data sentence $GPGSA.

The satellite geometry does not cause inaccuracies in the position determination that can be measured in meters. In fact the DOP values amplify other inaccuracies. High DOP values just amplify other errors more than low DOP values.

The error in the position determination caused by the satellite geometry also depends on the latitude of the receiver. This is shown below

in the two diagrams. The diagram on the left side shows the inaccuracy of the height (at the beginning of the curve with SA), recorded in Wuhan (China). Wuhan is situated on 30.5° northern latitude were ideal satellite constellation can be found at all time. The graph on the right side shows the same interval recorded by the Casey-Station in the Antarctica (66.3° southern latitude). Due to the satellite constellation from time to time the error is much larger. Additionally the falsification by the atmospheric effect gets more significant the closer the position is to the poles (for an explanation see "atmospheric effects <#atmospheric>").

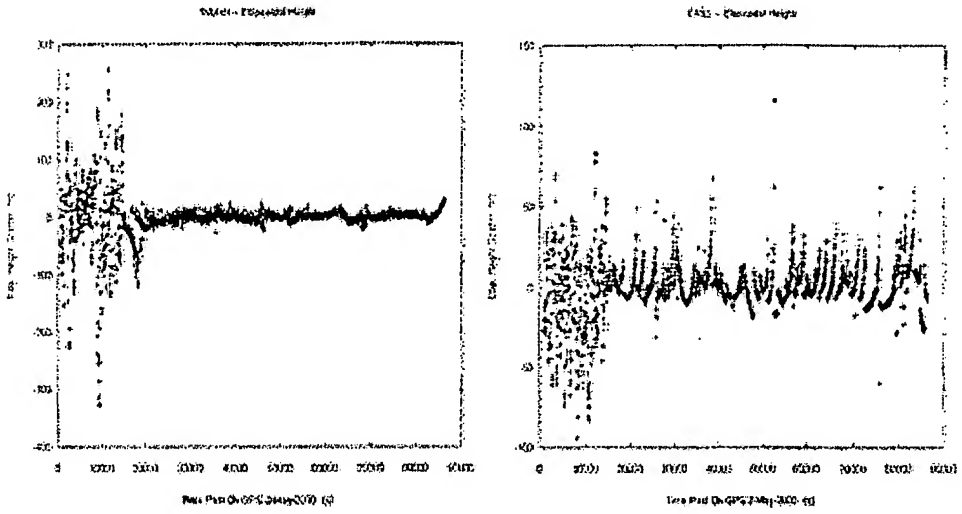

Error in the height determination at different latitudes
(Diagrams from http://www.ngs.noaa.gov/FGCS/info/sans_SA/world/ <http://www.ngs.noaa.gov/FGCS/info/sans_SA/world/>.
With friendly permission of Dr. Milbert (NOAA))

Satellite Orbits

Although the satellites are positioned in very precise orbits, slight shifts of the orbits are possible due to gravitation forces. Sun and moon have a weak influence on the orbits. The orbit data are controlled and corrected regularly and are sent to the receivers in the package of ephemeris data. Therefore the influence on the correctness of the position determination is rather low, the resulting error being not more than 2 m.

Multipath effect

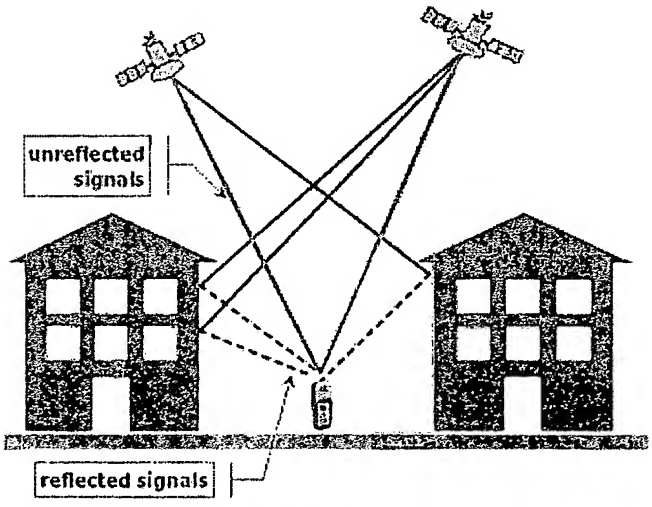

Interference caused by reflection of the signals

The multipath effect is caused by reflection of satellite signals (radio waves) on objects. It was the same effect that caused ghost images on television when antennae on the roof were still more common instead of todays satellite dishes.

For GPS signals this effect mainly appears in the neighbourhood of large buildings or other elevations. The reflected signal takes more time to reach the receiver than the direct signal. The resulting error typically lies in the range of a few meters.

Atmospheric effects

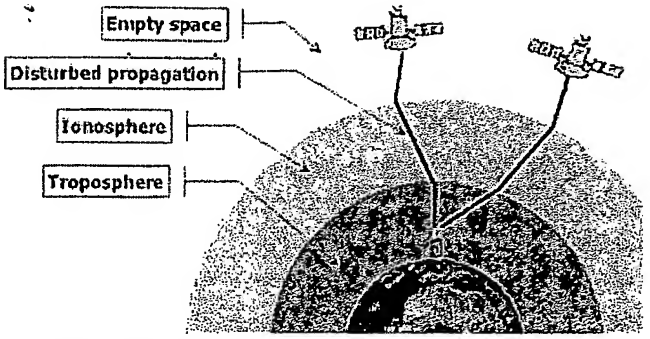

Influenced propagation of radio waves through the earth's atmosphere

Another source of inaccuracy is the reduced speed of propagation in the troposphere and ionosphere. While radio signals travel with the velocity of light in the outer space, their propagation in the ionosphere and troposphere is slower.

In the ionosphere in a height of 80 – 400 km a large number of electrons and positive charged ions are formed by the ionizing force of the sun. The electrons and ions are concentrated in four conductive layers in the ionosphere (D-, E-, F1-, and F2-layer). These layers refract the electromagnetic waves from the satellites, resulting in an elongated runtime of the signals.

These errors are mostly corrected by the receiver by calculations. The typical variations of the velocity while passing the ionosphere for low and high frequencies are well known for standard conditions. Theses variations are taken into account for all calculations of positions. However civil receivers are not capable of correcting unforeseen runtime changes, for example by strong solar winds.

It is known that electromagnetic waves are slowed down inversely proportional to the square of their frequency ($1/f^2$) while passing the ionosphere. This means that electromagnetic waves with lower frequencies are slowed down more than electromagnetic waves with higher frequencies. If the signals of higher and lower frequencies which reach a receiver are analysed with regard to their differing time of arrival, the ionospheric runtime elongation can be calculated. Military GPS receivers use the signals of both frequencies (L1 and L2) which are influenced in different ways by the ionosphere and are able to eliminate another inaccuracy by calculation.

The tropospheric effect is a further factor elongating the runtime of electromagnetic waves by refraction. The reasons for the refraction are different concentrations of water vapour in the troposphere, caused by different weather conditions. The error caused that way is smaller than the ionospheric error, but can not be eliminated by calculation. It can only be approximated by a general calculation model.

The following two graphs visualize the ionospheric error. The left data were collected with a one-frequency receiver without ionospheric correction, the right data were collected with a two-frequency receiver with ionospheric correction. Both diagrams have approximately the same scale (Left: latitude -15 m to +10 m, longitude -10 m to +20 m, Right: latitude -12 m to +8 m, longitude -10 m to +20 m). The right graph clearly shows less outliers, while the mean accuracy of the position for 95 % of the data is not considerably enhanced by the correction of the ionospheric error.

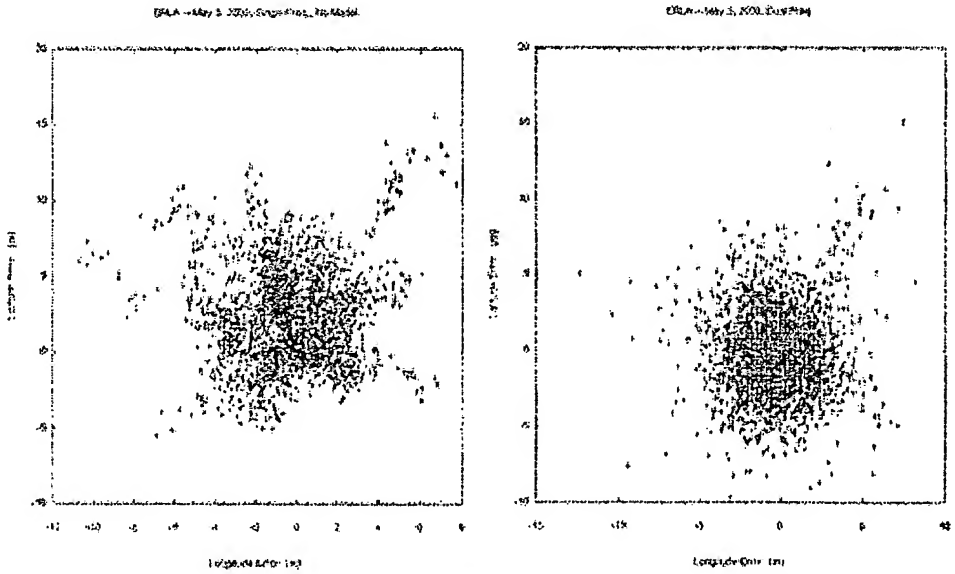

Position determination without and with atmospheric corrections by using the second frequency on a dual-frequency receiver (diagrams from http://www.ngs.noaa.gov/FGCS/info/sans_SA/iono <http://www.ngs.noaa.gov/FGCS/info/sans_SA/iono>. With friendly permission of Dr. Milbert (NOAA))

With the implementation of WAAS and EGNOS it s possible to set up „maps" of the atmospheric conditions over different regions. The correction data are sent to the receivers, enhancing the accuracy considerably.

Clock inaccuracies and rounding errors

Despite the synchronization of the receiver clock with the satellite time during the position determination, the remaining inaccuracy of the time still leads to an error of about 2 m in the position determination. Rounding and calculation errors of the receiver sum up approximately to 1 m:

Relativistic effects

The following section shall not provide a comprehensive explanation of the theory of relativity. In the normal life we are quite unaware of the omnipresence of the theory of relativity. However it has an influence on many processes, among them is the proper functioning of the GPS system. This influence will be explained shortly in the following.

As we already learned, the time is a relevant factor in GPS navigation and must be accurate to 20 - 30 nanoseconds to ensure the necessary accuracy. Therefore the fast movement of the satellites themselves (nearly 12000 km/h) must be considered.

Whoever already dealt with the theory of relativity knows that time runs slower during very fast movements. For satellites moving with a speed of 3874 m/s, clocks run slower when viewed from earth. This relativistic time dilation leads to an inaccuracy of time of approximately 7,2 microseconds per day (1 microsecond = 10^{-6} seconds).

The theory of relativity also says that time moves the slower the stronger the field of gravitation is. For an observer on the earth surface the clock on board of a satellite is running faster (as the satellite in 20000 km height is exposed to a much weaker field of gravitation than the observer). And this second effect is six times stronger than the time dilation explained above.

Altogether, the clocks of the satellites seem to run a little faster. The shift of time to the observer on earth would be about 38 milliseconds per day and would make up for an total error of approximately 10 km per day. In order that those error do not have to be corrected constantly, the clocks of the satellites were set to 10.229999995453 Mhz instead of 10.23 Mhz but they are operated as if they had 10.23 MHz. By this trick the relativistic effects are compensated once and for all.

There is another relativistic effect, which is not considered for normal position determinations by GPS. It is called Sagnac-Effect and is caused by the movement of the observer on the earth surface, who also moves with a velocity of up to 500 m/s (at the equator) due to the rotation of the globe. The influence of this effect is very small and complicate to calculate as it depends on the directions of the movement. Therefore it is only considered in special cases.

The errors of the GPS system are summarized in the following table. The individual values are no constant values, but are subject to variances. All numbers are approximative values.

Ionospheric effects	± 5 meters
Shifts in the satellite orbits	± 2.5 meter
Clock errors of the satellites' clocks	± 2 meter
Multipath effect	± 1 meter
Tropospheric effects	± 0.5 meter
Calculation- und rounding errors	± 1 meter

Altogether this sums up to an error of ± 15 meters. With the SA still activated, the error was in the range of ± 100 Meter. Corrections by systems like WAAS and EGNOS, which mainly reduce ionospheric effects, but also improve orbits and clock errors, the overall error is reduced to approximately ± 3 - 5 meters.

Transverse Fresnel-Fizeau drag effects in strongly dispersive media.

I. Carusotto,[1,*] M. Artoni,[2,3] G. C. La Rocca,[4] and F. Bassani[4]

[1] *Laboratoire Kastler Brossel, École Normale Supérieure, 24 rue Lhomond, 75231 Paris Cedex 05, France*

[2] *INFM, Department of Chemistry and Physics of Materials, Via Valotti 9, 25133 Brescia, Italy*

[3] *INFM, European Laboratory for non-Linear Spectroscopy, Via N. Carrara 1, 50019 Sesto Fiorentino, Italy.*

[4] *Scuola Normale Superiore and INFM, Piazza dei Cavalieri 7, I-56126 Pisa, Italy*

(Dated: June 9, 2003)

A light beam normally incident upon an uniformly moving dielectric medium is in general subject to bendings due to a transverse Fresnel-Fizeau light drag effect. In conventional dielectrics, the magnitude of this bending effect is very small and hard to detect. Yet, it can be dramatically enhanced in strongly dispersive media where slow group velocities in the m/s range have been recently observed taking advantage of the electromagnetically induced transparency (EIT) effect. In addition to the usual downstream drag that takes place for positive group velocities, we predict a significant anomalous upstream drag to occur for small and negative group velocities. Furthermore, for sufficiently fast speeds of the medium, higher order dispersion terms are found to play an important role and to be responsible for peculiar effects such as light propagation along curved paths and the restoration of the spatial coherence of an incident noisy beam. The physics underlying this new class of slow-light effects is thoroughly discussed.

PACS numbers: 42.50.Gy , 42.25.Bs

I. INTRODUCTION

A constant effort has always be devoted to the search for new effects and materials to control the propagation of light waves. Over the past few years, in particular, the use of quantum interference has led to an astonishing control of light waves propagating through specific classes of atomic and solid state media. These materials exhibit superior properties that cannot be found in conventional ones. *Slow light* propagation at group velocities as small as 1 m/s, e.g., has been observed in experiments with Bose-Einstein condensates of sodium atoms [1, 2], in hot rubidium vapors [3, 4] as well as in solid doped $Pr:Y_2SiO_5$ [5] crystals and Ruby [6]. Reversible *stopping* of a laser pulse [7] in ultracold and hot alkali vapors [8, 9] as well as in $Pr:Y_2SiO_5$ crystal has also been observed [5].

Light stopping and slow-light propagation effects originate from electromagnetically induced transparency (EIT). Such a widely discussed phenomenon arises from quantum interference and is characterized by a strong enhancement of the refractive index dispersion within a narrow frequency window around the medium resonance where absorption turns out to be largely quenched. The study of such a phenomenon goes back to the late seventies when non-absorbing resonances in atomic sodium have first been observed by Gozzini's group and later interpreted in terms of coherent population trapping [10, 11, 12].

The interest for such a phenomenon has revived [13] over the past decade and has now become a rather topical area of research [14, 15], much work being done on fundamental issues: high nonlinear coupling between weak fields and quantum entanglement of slow photons [16, 17, 18], entanglement of atomic ensembles [19], quantum memories [20] and enhanced acousto-optical effects [21], just to mention a few. In particular, a strict analogy between slow-light in moving media and light propagating in curved space-times has been unveiled and some of its consequences have been recently discussed [22, 23, 24, 25, 26, 27, 28].

Recently it has been also anticipated in [29] that EIT media are ideal candidates for the observation of extremely low and negative group velocities and (apparently) superluminal behaviour. In such media, the group velocity can in fact be readily tuned over a wide range of negative values directly by varying the coupling and probe detunings in a standard three-level Λ configuration.

Although most slow light and negative group velocity experiments have dealt with the basic problem of a light pulse delay during its propagation across the dispersive medium, ultraslow positive or negative group velocities can have interesting consequences in many different scenarios. In this paper we present a thorough investigation of slow-light propagation through a moving medium. Specifically, we examine a configuration in which a highly dispersive EIT medium which moves with uniform velocity and normally [1] to an incident light beam of finite spa-

* Electronic address: Iacopo.Carusotto@lkb.ens.fr

[1] A configuration in which the medium is set to move parallel to the probe light-beam, leading to the more familiar *longitudinal* Fresnel-Fizeau effect, has been studied in [30]. Also in this configuration, the magnitude of the light-drag effect is predicted to

tial extent. The same geometry was adopted in the early seventies by Jones in his pioneering work on the *transverse* Fresnel-Fizeau light drag effect [31, 32] leading to the observation of a very small downstream bending, i.e., in the direction of motion, of a light ray. The use of a strongly dispersive medium supporting slow light, rather than the non-dispersive glassy material used by Jones, will not only allow for a remarkable enhancement of the drag effects but also for qualitatively new features.

The possibility of having light propagating with small negative group velocities across the dragging medium is predicted to yield large *upstream* light bendings, i.e. in the direction opposite to that of the medium. The phenomenology of such an a anomalous Fresnel-Fizeau light drag effect, which has been the subject of an old controversy during the late seventies [33, 34], is here discussed in detail unwinding some of its controversial aspects.

For sufficiently fast dragging speeds, the correct description of the slow light transverse dragging effect requires that absorption dispersion and group velocity dispersion be taken into account. As we shall see below, it turns out that these higher–order dispersion terms introduce new and peculiar features, such as propagation along curved light paths and the restoration of the spatial coherence of a noisy beam. All the numerical results presented in this paper have been obtained using realistic parameters taken from slow-light experiments in ultracold atomic clouds [1]. Since the physics of the system is essentially determined by the electromagnetically induced transparency effect, the physical features here discussed are however extremely general and hold through also for the recently prepared solid state EIT media.

The paper is organized as follows. In sec. II we introduce the physical system and we present the model used for our predictions. The general theory of the transverse Fresnel-Fizeau light drag effect is presented in sec. III. These general results are specialized to the case of a strongly dispersive dressed medium driven into a Λ configuration by a resonant and non-resonant coupling beam respectively in sec. IV and in sec. V: in the former case, the group velocity is small and positive, so the transverse Fresnel drag occurs in the usual downstream direction; in the latter case, the negative group velocity is shown to give an anomalous upstream Fresnel drag. In sec.VI we proceed to discuss some effects which arise from the inclusion of higher order dispersion terms. We carry out a complete analysis for two specific instances. In one case, the beam spectrum reshaping due to absorption and group velocity dispersion, which makes the average group velocity to bend during propagation, is seen to lead to curved light paths. In the other, the frequency dispersion of absorption is seen to act as a filter for spatial fluctuations of the beam, whose space coherence properties improve as it propagates through the medium. Finally, a summary of the work is given in sec.VII where conclusions are also drawn.

be strongly enhanced in the slow light regime.

II. THE MODEL AND GENERAL THEORY

We consider a monochromatic *probe* light beam of frequency ω_0 propagating along the z axis and normally incident upon a homogeneous dielectric medium uniformly moving along the x direction as shown in fig.1. We here denote with L the thickness of the slab and with v its velocity $v \ll c$. The probe beam has a Gaussian profile centered in (x_0, y_0) so that at $z = 0$ one has,

$$E_0(x,y) = E_0\, e^{-[(x-x_0)^2+(y-y_0)^2]/2\sigma_0^2}, \qquad (1)$$

where σ_0 is the beam waist. The corresponding Fourier transform $\tilde{E}_0(k_x, k_y)$ of $E_0(x,y)$ is then a Gaussian of width σ_0^{-1}.

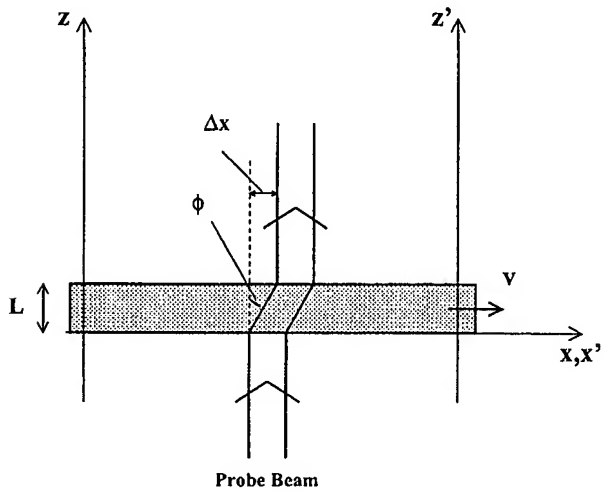

FIG. 1: Scheme of the experimental set-up under consideration.

In the following we shall always restrict our attention to the case of a weak probe beam, which allows us to apply linear response theory and describe the polarization of the medium by means of a dielectric function ϵ. Assuming for simplicity a non-magnetic ($\mu = 1$) and isotropic $\epsilon_{i,j} = \epsilon\,\delta_{i,j}$ medium, the scalar dielectric function ϵ completely characterizes the linear polarization of the medium in its rest frame Σ'. Spatial locality of the dielectric polarization will also be assumed, i.e. ϵ will be taken to depend on the frequency ω' but not on the wavevector k'. Primed quantities will refer to the medium rest frame Σ', while the non-primed ones will refer to the laboratory frame Σ. The linearity of the optical response and the translational invariance of the system on the (x,y) plane allow us to decompose the incident field in its Fourier components in the (x,y) plane, to propagate each of them independently from the others, and to

finally reconstruct the transmitted beam profile by using an inverse Fourier transform.

In the Σ' frame, the dispersion law inside the medium has the usual form:

$$\epsilon(\omega')\,\omega'^2 = c^2(k_x'^2 + k_y'^2 + k_z'^2). \tag{2}$$

Since the slab speed $v \ll c$, the linearized form of the Lorentz transformations can be used, namely:

$$\omega' = \omega - k_x v \tag{3}$$

$$k_x' = k_x - \frac{\omega}{c^2} v \tag{4}$$

$$k_{y,z}' = k_{y,z}. \tag{5}$$

Notice that even though the medium does exhibits no spatial dispersion in its rest frame Σ', spatial dispersion arises however in the laboratory frame Σ from the dependence of ω' on k_x [2]. By inserting the transformations (3-5) into the dispersion law (2), one obtains the following expression:

$$\frac{(\omega - k_x v)^2}{c^2}\,\epsilon(\omega - k_x v) = \left(k_x - \frac{\omega v}{c^2}\right)^2 + k_y^2 + k_z^2. \tag{6}$$

This equation represents the dispersion law in Σ and can be used to determine the propagation of the light beam across the slab. Knowing the frequency ω_0 and the transverse components $k_{x,y}$ of the wavevector allows us to obtain from (6) the z component $k_z^{(in)}$ of the wave-vector inside the medium:

$$k_z^{(in)}(k_x, k_y) = $$

$$= \sqrt{\left(\frac{\omega_0 - k_x v}{c}\right)^2 \epsilon(\omega_0 - k_x v) - \left(k_x - \frac{\omega_0 v}{c^2}\right)^2 - k_y^2}, \tag{7}$$

as well as in the external free space:

$$k_z^{(out)}(k_x, k_y) = \sqrt{\frac{\omega_0^2}{c^2} - k_x^2 - k_y^2}. \tag{8}$$

The profile of the transmitted beam can then be obtained by decomposing the field in its Fourier components at transverse wavevector (k_x, k_y) and propagating each of them independently with the wave-vectors (7) and (8). Since the energy flux must be along the positive z axis, the roots with positive real part $\mathrm{Re}[k_z^{(in,out)}] > 0$ have to be taken [3].

For each component, the amplitude at the position $0 \le z \le L$ inside the slab is given by:

$$\tilde{E}(k_x, k_y; z) = e^{i\Phi(k_x, k_y; z)}\,\tilde{E}_0(k_x, k_y) \tag{9}$$

with a phase Φ:

$$\Phi(k_x, k_y; z) = k_z^{(in)}(k_x, k_y)\,z \tag{10}$$

Notice that the wavevector $k_z^{(in)}(k_x, k_y)$ as well as the phase $\Phi(k_x, k_y; z)$ are generally complex quantities; their imaginary parts vanish only for non-absorbing, non-amplifying medium. Past the slab, the transmitted amplitude at the position $z > L$ is given by the same equation (9) with the phase Φ now given by:

$$\Phi(k_x, k_y; z) = k_z^{(in)}(k_x, k_y)\,L + k_z^{(out)}(k_x, k_y)\,(z - L). \tag{11}$$

The spatial profile of the transmitted beam at any point z can then be obtained taking the inverse Fourier transform of (9),

$$E(x, y, z) = \int \frac{dk_x\,dk_y}{2\pi}\, e^{i(k_x x + k_y y)}\, e^{i\Phi(k_x, k_y; z)}\,\tilde{E}_0(k_x, k_y). \tag{12}$$

III. THE TRANSVERSE FRESNEL-FIZEAU DRAG EFFECT

Provided that the incident beam waist σ_0 is wide enough, only a very small window of wave-vectors (k_x, k_y) around $k_{x,y} = 0$ is effectively relevant to the propagation dynamics and one can safely expand the phase (11) in powers of $k_{x,y}$ so that to the lowest order one has:

$$\Phi(k_x, k_y; z) = \frac{\omega_0}{c}\sqrt{\epsilon(\omega_0)}\left[1 - \frac{k_x v}{\omega_0}\left(1 - \frac{1}{\epsilon(\omega_0)}\right) - \frac{k_x\,v}{2\,\epsilon(\omega_0)}\frac{d\epsilon}{d\omega}\right] L + \frac{\omega_0}{c}(z - L). \tag{13}$$

The position of the center (x_c, y_c) of the resulting wave packet at a given z can be obtained inserting the expansion (13) into (12) and then invoke the so-called *stationary-phase* principle. This states that the integral in (12) has its maximum value at those points (x_c, y_c) for which constructive interference between the different Fourier components occurs, that is at those points at which the phase of the integrand is stationary [35]:

$$\frac{\partial}{\partial k_{x,y}}\left(\mathrm{Re}[\Phi(k_x, k_y; z)] + k_x x_c + k_y y_c\right)\Big|_{k_x = k_y = 0} = 0. \tag{14}$$

Inserting into (14) the expression of the phase (13) and assuming the imaginary part ϵ_i of $\epsilon = \epsilon_r + i\,\epsilon_i$ to be negligible, one finds that in the laboratory frame Σ the beam

---

[2] In the rest frame Σ', the dielectric polarization of a medium with frequency dispersion depends on the retarded values of the electric field at the same spatial position. As seen from the laboratory frame Σ, the polarization at a given point will thus depend on the electric field at different spatial positions, which means that a moving medium shows a spatial dispersion in Σ even if it is only temporally dispersive in the rest frame Σ'.

[3] As the reflection amplitude is proportional to $\epsilon - 1$, the approximation of neglecting interface reflections is a reasonable approximation in the case of an ultra cold atomic gas on which the present paper is focussed. On the other hand, a more complete theory including the possibility of multiple interface reflections is required in the case of a solid state medium.

propagates inside the moving slab at a non-vanishing angle θ with respect to the normal z direction given by:

$$\tan\theta = \frac{v}{c}\left[\sqrt{\epsilon_r(\omega_0)} + \frac{\omega_0}{2\sqrt{\epsilon_r(\omega_0)}}\frac{d\epsilon_r}{d\omega} - \frac{1}{\sqrt{\epsilon_r(\omega_0)}}\right] = \\ = \frac{v}{c}\left[\frac{c}{v'_{\rm gr}} - \frac{v'_{\rm ph}}{c}\right]. \quad (15)$$

Here $v'_{\rm gr}$ and $v'_{\rm ph}$ denote respectively the group and phase velocities in the medium rest frame Σ':

$$v'_{\rm ph} = \frac{c}{\sqrt{\epsilon_r(\omega_0)}} \quad (16)$$

$$v'_{\rm gr} = \frac{c}{\sqrt{\epsilon_r(\omega_0)} + \frac{\omega_0}{2\sqrt{\epsilon_r(\omega_0)}}\frac{d\epsilon_r}{d\omega}}. \quad (17)$$

This deflection of the light beam can be interpreted as a *transverse* Fresnel-Fizeau drag effect, in which the beam of light is dragged by the transverse motion of the medium. After exiting from the rear surface of the slab, the beam again propagates along the normal direction. Its center, however, turns out to be laterally shifted by an amount,

$$\Delta x = Lv\left[\frac{1}{v'_{\rm gr}} - \frac{v'_{\rm ph}}{c^2}\right]. \quad (18)$$

along a direction parallel to the medium velocity. This expression is in agreement with the ones derived by Player and by Rogers [36, 37].

While the group velocity direction inside the moving medium makes a finite angle θ with respect to the normal, the transverse x and y components of the phase velocity are always vanishing in the laboratory frame Σ because the light beam is normally incident on the slab and the transverse wave vector is conserved at the interface. The non-parallelism of the group and phase velocities arises then from the effective spatial dispersion acquired in the laboratory frame Σ by the moving medium [4]. Indeed, one can calculate the group velocity $\mathbf{v_{gr}} = \nabla_{\mathbf{k}}\omega(\mathbf{k})$ at $k_{x,y} = 0$ directly from the dispersion law (6) to obtain for each component:

$$v_{{\rm gr},x} = v\left(1 - \frac{1}{\epsilon + \frac{\omega}{2}\frac{d\epsilon}{d\omega}}\right) = v\left(1 - \frac{v'_{\rm gr}\,v'_{\rm ph}}{c^2}\right) \quad (19)$$

$$v_{{\rm gr},y} = 0 \quad (20)$$

$$v_{{\rm gr},z} = \frac{c}{\sqrt{\epsilon} + \frac{\omega}{2\sqrt{\epsilon}}\frac{d\epsilon}{d\omega}} = v'_{\rm gr}. \quad (21)$$

The non-vanishing value of $v_{{\rm gr},x}$ is responsible for the transverse Fresnel-Fizeau drag. The value of $\tan\theta = v_{{\rm gr},x}/v_{{\rm gr},z}$ obtained from (19) and (21) agrees indeed with (15).

Another picture of this drag effect can be obtained by working in the rest frame Σ' [38]. Because of the aberration of light [35], the direction of the incident beam makes an angle $\theta'_{\rm inc} = -v/c$ with the normal [5]. In the rest frame Σ', the group and phase velocities inside the medium are parallel to each other and make an angle $\theta'_{\rm refr} = -v/(c\sqrt{\epsilon})$ with the normal according to Snell's law. The modulus of the group velocity in Σ' is given by (17). By Lorentz-transforming back the group velocity to the laboratory frame Σ, it is easy to check that the same deflection angle as in (15) is obtained.

As one can see from the explicit expression (18) the magnitude of the transverse drag Δx is largest for a strongly dispersive medium in which ϵ has a rapid frequency dependence and the group velocity $v'_{\rm gr}$ results much slower than the vacuum speed of light $v'_{\rm gr} \ll c$.

In this case, Galilean velocity composition laws can be safely applied and the result (18) simplifies to

$$\Delta x = \frac{Lv}{v'_{\rm gr}}, \quad (22)$$

which yields a very intuitive interpretation for Δx as the displacement of the medium during the time interval $\Delta t = L/v'_{\rm gr}$ taken by the light to travel across it.

IV. THE TRANSVERSE FRESNEL-FIZEAU DRAG EFFECT IN A EIT MEDIUM

The first experimental observation of the transverse Fresnel-Fizeau drag effect was performed in the mid-1970's by Jones [31] using a rotating glass disk as moving dielectric medium. In such a non-dispersive medium the phase and group velocities were of the order of c ($c/v'_{\rm gr} \approx c/v'_{\rm ph} \approx 1.5$) and the limited rotation velocity of the disk at the laser spot ($v \simeq 2\times10^4$cm/s) limited the lateral displacement to a distance of the order of 6 nm. However, a clever optical alignment technique allowed not only to observe the effect, but also to discriminate the validity of the result (15) from other possible expressions [32].

As remarked in the previous section, the use of a strongly dispersive medium allows for a significant enhancement of the drag effect. Very slow group velocities can now be obtained in both atomic samples [1, 2, 3, 4] and solid-state media [5, 6] by optically dressing a resonant transition with a coherent *coupling* laser beam as shown in the Λ level scheme of fig.2.

Under the assumption of a weak probe beam, linear response theory holds for the system dressed by the

[4] The assumed isotropy of the medium in its rest frame Σ' guarantees that group and phase velocities are always parallel in Σ'.

[5] Notice that in the rest frame Σ', the beam waist appears as uniformly translating along the negative x axis. This unfamiliar feature however does not affect the argument.

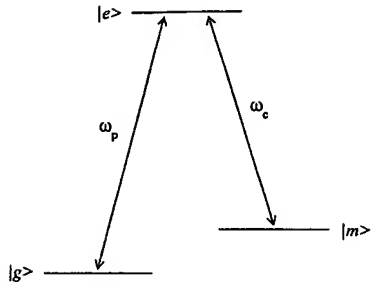

FIG. 2: Scheme of the energy levels involved in the optical transitions.

strong coupling beam: the resulting dielectric constant is to be interpreted as describing the linear response of the optically driven medium to the weak probe. Obviously, this dressed dielectric constant has a strongly nonlinear dependence on the coupling intensity so to account for all the nonlinear processes induced in the medium by the coupling field. In the simplest case of non-degenerate levels, the rest frame dielectric constant of our optically driven Λ configuration acquires the well-known form [11, 12, 13, 14],

$$\epsilon(\omega) = \epsilon_\infty + \frac{4\pi f}{\omega_e - \omega - i\gamma_e/2 - \frac{|\Omega_c|^2}{\omega_m+\omega_c-\omega-i\gamma_m/2}} \qquad (23)$$

where $\omega_{e(m)}$ and $\gamma_{e(m)}$ are respectively the frequency and the linewidth of the excited e and metastable m states, where we have set $\omega_g = 0$. Here ω_c is the frequency of the $e \leftrightarrow m$ coherent coupling beam [6] and Ω_c its Rabi frequency. The linewidth γ_m of the metastable state is much smaller than the linewidth γ_e of the excited state. The f parameter quantifies the oscillator strength of the optical transition: for an ultra cold atomic gas [1] at atomic densities $n \approx 10^{12}\,\mathrm{cm}^{-3}$, f is of the order of a few $10^{-3}\gamma_e$. The background dielectric constant ϵ_∞ takes into account the effect of all the other non-resonant transitions and for an atomic gas can be taken to be 1 to a very good approximation.

For a resonantly dressed medium, i.e. $\delta_c = \omega_c - (\omega_e - \omega_m) = 0$, the dielectric function (23) in the neighborhood of the resonance $|\omega - \omega_e| \ll \gamma_e$ can be rewritten as:

$$\epsilon(\omega) = \epsilon_\infty + \frac{8\pi f i}{\gamma_e}\left[1 + \frac{2i\Omega_c^2/\gamma_e}{\omega_e - \omega - \frac{i}{2}(\gamma_m + \frac{4\Omega_c^2}{\gamma_e})}\right]. \qquad (24)$$

In the imaginary part of this expression shown in fig.3a, it is easy to seize a narrow dip around $\omega = \omega_e$ in the otherwise wide absorption profile of the $g \to e$ transition. Provided $\Omega_c^2/\gamma_e \gg \gamma_m$, absorption at the center of the dip is strongly suppressed, yielding nearly perfect transparency for a resonant probe beam; this effect is the so-called *electromagnetically induced transparency* (EIT) effect [10]. The linewidth of the dip is $\Gamma \simeq 4\Omega_c^2/\gamma_e$ and becomes strongly sub-natural ($\Gamma \ll \gamma_e$) for $\Omega_c \ll \gamma_e$. The assumed inequality $\gamma_m \ll \gamma_e$ guarantees that a good level of transparency can be obtained simultaneously with a sub-natural linewidth of the dip.

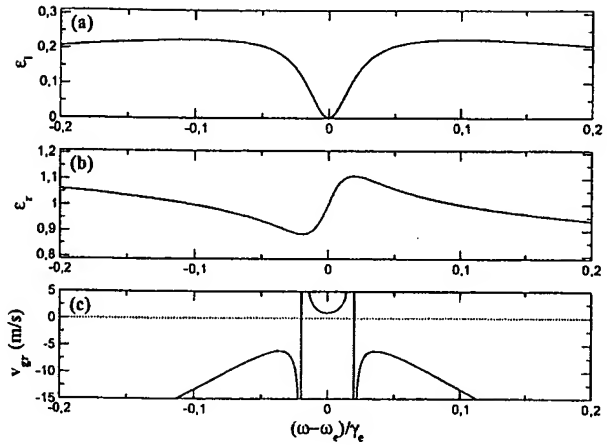

FIG. 3: Resonantly dressed EIT medium at rest: plot of the imaginary (a) and real (b) parts of the dielectric function ϵ and of the group velocity v_{gr} (c). Medium parameters correspond to the case of an ultra cold ^{23}Na gas: $\gamma_e \simeq 2\pi \cdot 10$ MHz, $\lambda_e = 589\,\mathrm{nm}$, $f = 0.009\,\gamma_e$, $\epsilon_\infty = 1$, $\gamma_m = 10^{-4}\gamma_e$. The Rabi frequency of the resonant ($\delta_c = 0$) coupling beam is $\Omega_c = 0.1\,\gamma_e$. For this choice of parameters, the minimum (positive) group velocity is $v_{gr} \approx 1\,\mathrm{m/s}$.

In the dip region, the real part (fig.3b) of the dielectric function (23) shows an extremely steep dispersion yielding the group velocity:

$$\frac{v_{gr}}{c} \simeq \frac{|\Omega_c|^2}{2\pi f \omega_e} \qquad (25)$$

which can be orders of magnitude slower than the vacuum value c (fig.3c). This suggests that the importance of the transverse Fresnel-Fizeau drag effect (18) should be strongly enhanced in an EIT medium.

To verify this prediction, a complete calculation of the profile of the transmitted probe beam can be numerically performed by inserting the explicit expression of the dielectric function (23) into the dispersion law (6) and then performing the inverse Fourier transform (12). For a probe exactly on resonance with the $g \to e$ transition ($\omega_0 = \omega_e$), the numerical result plotted in fig.4a is in perfect agreement with the analytic prediction (18) when the value (25) for the group velocity is used. The near absence of absorption at the center of the dip guarantees that only a small fraction of the incident probe intensity is absorbed by the medium (fig.4b).

[6] Doppler shift of the coupling beam is avoided by choosing the direction of the coupling beam to be orthogonal to both the probe beam and the medium velocity. The waist of the coupling beam is taken as much larger than both the waist σ_0 of the probe and the thickness L of the medium.

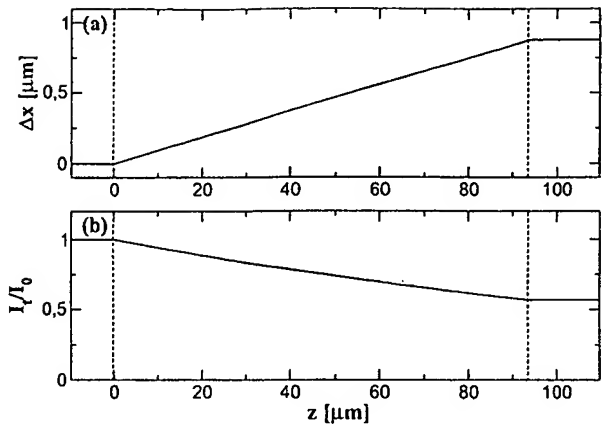

FIG. 4: Propagation of a light beam through a slowly moving ($v = 0.01$ m/s), resonantly dressed EIT medium. The optical parameters of the medium are the same as in fig.3, the vertical dashed lines correspond to the surfaces of the medium, whose thickness is taken as $L = 93\,\mu$m. The incident beam is resonant $\omega_0 = \omega_e$ and its waist is $\sigma_0 = 20\,\mu$m. *Downstream* transverse Fresnel-Fizeau drag (a) and corresponding weak absorption of the beam (b). The x axis is oriented in the downstream direction.

Group velocities as low as 1 m/s have been observed in ultra cold atomic gases. For the choice of parameters ($v_{\rm gr} = 1$ m/s and $L \approx 100\,\mu$m) made in fig.4, a medium velocity of the order of $v = 0.01$ m/s gives a lateral shift of the order of $\Delta x \approx 1\,\mu$m, orders of magnitude larger than the one originally observed by Jones [31, 32]. An even larger lateral shift Δx should be obtained by using a solid state material as dragging medium. Group velocities as slow as $v_{\rm gr} = 45$ m/s have in fact been recently observed in a Pr doped Y_2SiO_5 [5] and Ruby [6] crystals. Furthermore, the mechanical rigidity and the possibility of working at higher temperatures should allow one to study the drag effect on a thicker sample moving at a higher speed v.

V. ANOMALOUS TRANSVERSE FRESNEL-FIZEAU DRAG EFFECT

The discussion of the previous sections has focused on the most common case of media with *normal* dispersion. As Kramers-Kronig causality relations [39] ensure that

$$\frac{c}{v_{\rm gr}} - \frac{v_{\rm ph}}{c} > 0, \qquad (26)$$

for all frequency regions at which the medium is transparent and non-amplifying, the corresponding transverse Fresnel-Fizeau drag (18) results directed in the *downstream* direction, as if the light were to be dragged by the moving medium.

On the other hand, several papers during the 70's [33, 34] have discussed the possibility of having an *upstream* transverse Fresnel-Fizeau drag in the presence of *anomalous* dispersion, i.e. in the presence of negative group velocity. As negative group velocities in non-magnetic media are forbidden by Kramers-Kronig relations [39] in all frequency regions where the medium is transparent and non-amplifying, it has been possible to observe negative group velocities only in the presence of substantial absorption [40, 41, 42] or in amplifying media [43]. Notice that the negative group velocity effects which can be observed in left-handed media even in the absence of absorption arise from a completely different mechanism, that is from a simultaneously negative value of both the dielectric constant ϵ and the magnetic susceptibility μ [44]. This class of effects are excluded from the present discussion, which is limited to non-magnetic ($\mu = 1$) materials.

In all experiments performed up to now, negative group velocities have been demonstrated by observing that the pulse advances in time with respect to the same wave packet propagating in vacuum. This kind of apparently superluminal behavior obviously refers to the peak of the wave packet only, and not to the propagation velocity of information; as discussed in the review [45], the velocity of the front of a step-function signal can never exceed c.

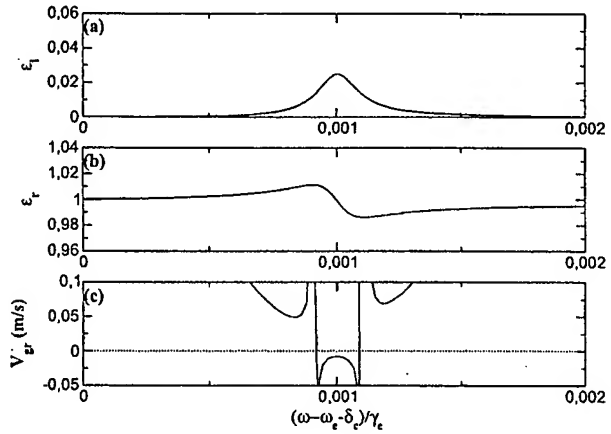

FIG. 5: Plot of the imaginary part $\epsilon_i(\omega)$ of the dielectric function (a), of its real part $\epsilon_r(\omega)$ (b), and of the group velocity $v_{\rm gr}(\omega)$ (c) for a non-resonantly ($\delta_c = 10\gamma_e$) dressed EIT medium at rest. The other parameters are the same as in fig.3.

As we have recently anticipated in [38], a significant upstream Fresnel-Fizeau drag effect should be observable in non-resonantly dressed EIT media, when the coupling beam is not exactly on resonance with the $m \to e$ transition, but has a finite detuning $|\delta_c| = |\omega_m + \omega_c - \omega_e| \geq \gamma_e$. This kind of media have in fact been shown to be good candidates for the observation of ultra slow and negative group velocities [29]. In the case $|\delta_c| \gg \gamma_e$, the dielectric function (23) in the neighborhood of $\omega = \omega_m + \omega_c$ (fig.5)

can be written in the Lorentzian form:

$$\epsilon(\omega) = \epsilon_\infty - \frac{4\pi f}{\delta_c} + \frac{4\pi f \Omega_c^2}{\delta_c^2} \frac{1}{\omega_2 - \omega - \frac{i}{2}(\gamma_m + \frac{\Omega_c^2 \gamma_e}{\delta_c^2})}. \tag{27}$$

Largest absorptions occur at the Raman resonance with the two-photon transition from the ground g state to the metastable m state via the excited e state, i.e. at the two-photon resonance frequency

$$\omega_2 = \omega_m + \omega_c + \frac{\Omega_c^2}{\delta_c}. \tag{28}$$

The shift Ω_c^2/δ_c from the bare resonant frequency is due to the optical Stark effect induced by the coupling beam. The linewidth of the resonance line is the sum of the bare linewidth of the metastable m level plus a contribution which takes into account its decay via the excited e state:

$$\gamma_2 = \gamma_m + \frac{\Omega_c^2}{\delta_c^2}\gamma_e. \tag{29}$$

For large coupling beam detunings $|\delta_c| \gg \Omega_c$, the linewidth γ_2 results much smaller than the natural linewidth of the excited state, while the oscillator strength of the transition is itself weakened:

$$f_2 = \frac{\Omega_c^2}{\delta_c^2} f. \tag{30}$$

The peak absorption (proportional to f_2/γ_2) does not vary for increasing values of $|\delta_c|/\Omega_c$, at least as far as $\gamma_2 \gg \gamma_m$. On the other hand, the anomalous dispersion at resonance $\omega = \omega_2$ is under the same conditions enhanced due to the narrower linewidth γ_2. The corresponding group velocity is given by

$$\frac{v_{gr}}{c} = -\frac{\delta_c^2}{8\pi f \omega_e \Omega_c^2}\left(\gamma_m + \frac{\Omega_c^2}{\delta_c^2}\gamma_e\right)^2 \tag{31}$$

which, in the limit $\gamma_2 \gg \gamma_m$, is a factor $\gamma_e^2/4\delta_c^2$ slower in magnitude than the one obtained in the resonant $\delta_c = 0$ case considered in the previous section. This means that the use of a detuned coupling with $|\delta_c| > \gamma_e$ should enable one to observe significant upstream drags over an optical thickness L of the order of the absorption length, so that the transmitted probe intensity still remains an appreciable fraction of the incident one.

In order to verify this expectation, we have again inserted the explicit expression of the dielectric function (23) into the propagation equation (6) and we have numerically performed the inverse Fourier transform so as to obtain the profile of the transmitted beam (fig.6a). As expected, light bendings are found to occur in the upstream direction and the magnitude of the effect is in good agreement with the approximated analytical expression (18) in which the imaginary part of ϵ was neglected. We have also verified in fig.6b that the beam

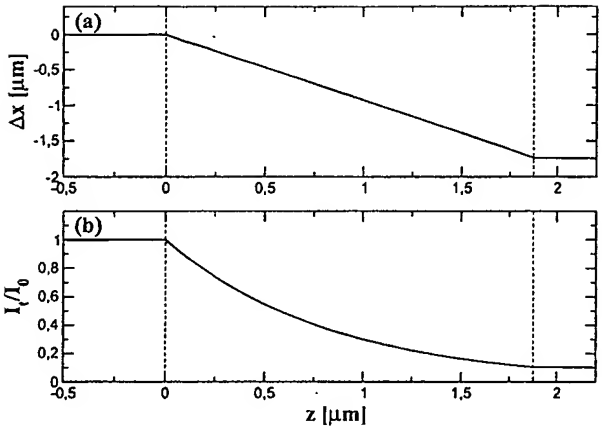

FIG. 6: Propagation of a light beam through a slowly moving ($v = 0.01$ m/s), non-resonantly dressed ($\delta_c = 10\,\gamma_e$) EIT medium; probe frequency on resonance with the two-photon transition ($\omega_0 = \omega_2$). The optical parameters of the medium are the same as in fig.5; the vertical dashed lines correspond to the surfaces of the medium, whose thickness is taken as $L = 1.9\,\mu$m. The incident beam waist is $\sigma_0 = 20\,\mu$m. Anomalous *upstream* transverse Fresnel-Fizeau drag (a) and corresponding absorption of the beam (b). The x axis is oriented in the downstream direction.

is not completely absorbed during propagation through the medium. Notice that for the same set of material parameters and the same experimental configuration as in the previous section, except for the coupling beam detuning δ_c, the group velocity $|v_{gr}|$ is now of the order of 0.01 m/s, i.e. a factor 100 slower than in the case of a resonant coupling. This explains the bigger deflection angle θ.

Non-resonantly dressed EIT media are therefore good candidates for the experimental observation of significant upstream deflections and consequently large anomalous transverse Fresnel-Fizeau drags. Such an observation should finally resolve a controversy started in the seventies about the possibility of such an effect [33, 34]. Furthermore, the anomalous upstream Fresnel-Fizeau drag could also provide an interesting way of demonstrating negative group velocities, in alternative to the usual [40, 41, 42, 43] measurement of the negative temporal delay of the pulse after its propagation across the medium.

VI. HIGHER ORDER DISPERSION EFFECTS

The effects discussed in the previous sections entirely rely on the strongly reduced value of the group velocity of light in EIT media. For slow enough medium velocities, higher order dispersion effects such as the dispersion of absorption or the group velocity dispersion are indeed very small and can be hardly observed in the results plotted in figs.4 and 6. On the other hand, these terms may

be no longer negligible for sufficiently large values of the medium velocity, regime in which the light propagation can exhibit qualitatively new features [7]. In the following of this section we shall discuss in detail two examples of such effects.

A. Light propagation along a curved path

In the present subsection, we shall discuss the effect of non-rectilinear light propagation due to simultaneously large dispersions of both absorption [46] (proportional to $d\epsilon_i/d\omega$) and group velocity (proportional to $d^2\epsilon_r/d\omega^2$).

For large enough values of the absorption dispersion $d\epsilon_i/d\omega$, the absorption coefficient can have significant variations across the range of transverse k_x vectors present in the incident beam. In this case, the center of mass of the k_x wave-vector distribution

$$k_x^{\rm cm}(z) = \frac{\int dk_x\, dk_y\, k_x\, |\tilde{E}(k_x,k_y;z)|^2}{\int dk_x\, dk_y\, |\tilde{E}(k_x,k_y;z)|^2} \qquad (32)$$

moves from its initial value $k_x^{\rm cm}(z=0)=0$ as the beam propagates through the medium. For a spatially wide Gaussian incident beam, we can limit the expansion of ϵ_i to the linear terms in $k_{x,y}$ and we find that the distribution of transverse wave vectors keeps a gaussian shape, but its center of mass $k_x^{\rm cm}(z)$ shifts to:

$$k_x^{\rm cm}(z) = -\frac{z}{\sigma_0^2}\frac{\partial {\rm Im}[k_z^{(\rm in)}]}{\partial k_x} \qquad (33)$$

For a negative value of $\partial {\rm Im}[k_z^{(\rm in)}]/\partial k_x$, the $k_x>0$ components result in fact less absorbed than the $k_x<0$ ones so that the Gaussian spectrum shifts towards the $k_x^{\rm cm}>0$ region; vice versa for a positive value of $\partial {\rm Im}[k_z^{(\rm in)}]/\partial k_x$.

In the slow group velocity regime ($v'_{\rm gr} \ll c$), the dependence of the propagation wavevector (7) on the transverse wave vector $k_{x,y}$ mainly comes from the Doppler effect combined with the strong frequency dispersion of the dielectric function, so that the transmission phase reads as:

$$\Phi(k_x,k_y;z) \simeq \frac{\omega_0\, z}{c}\sqrt{\epsilon(\omega_0 - k_x v)}. \qquad (34)$$

By applying the same stationary-phase arguments used in sec.III to the finite $k_x^{\rm cm}(z)$ case, we find that after propagation for a distance z the spatial center of mass of the beam is located at

$$\Delta x(z) = z\frac{v}{v'_{\rm gr}(\omega_0 - v\, k_x^{\rm cm}(z))}. \qquad (35)$$

In physical terms, as the spectral center of mass $k_x^{\rm cm}$ of the beam varies with z because of the filtering action of the absorption, the transverse Fresnel-Fizeau drag at a given position z has to be evaluated using the group velocity $v'_{\rm gr}$ at the Doppler shifted frequency $\omega_0 - v\,k_x^{\rm cm}(z)$. In the presence of group velocity dispersion, the variation of $k_x^{\rm cm}(z)$ with z implies that the light beam is no longer rectilinear, but acquires a finite curvature. Notice in particular that the analytical expression for the angle $\theta(z)$ between the trajectory (35) and the normal z direction

$$\tan\theta(z) = \frac{\partial \Delta x(z)}{\partial z} = $$
$$= \frac{v}{v'_{\rm gr}(\omega_0 - v k_x^{\rm cm})} + \frac{v^2\, z}{\left[v'_{\rm gr}(\omega - v k_x^{\rm cm})\right]^2}\frac{dv'_{\rm gr}}{d\omega}\frac{dk_x^{\rm cm}}{dz} \qquad (36)$$

now contains a term explicitly depending on the spectral center of mass shift $dk_x^{\rm cm}/dz$ which was not present in (15).

A related effect was discussed in the time domain in [47] where a small time-dependence of the group velocity for a light pulse propagating through a dispersive dielectric was predicted to show up as a consequence of the combined effect of the frequency dispersions of absorption and of group velocity.

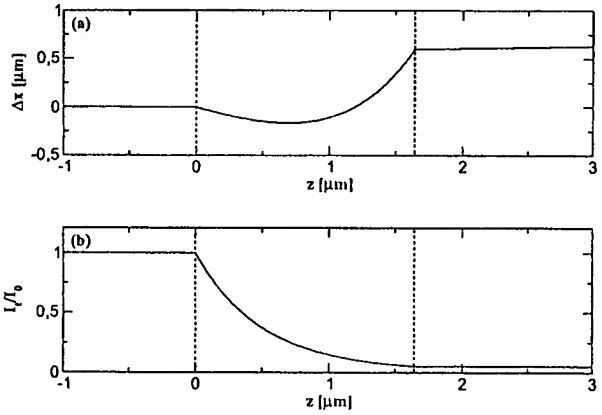

FIG. 7: Non-rectilinear light beam propagation through a moving (v = 4 m/s) EIT medium for a resonant coupling ($\delta_c = 0$) and a slightly detuned probe ($\omega_0 - \omega_e = 0.04\,\gamma_e$); the incident beam waist is $\sigma_0 = 3\,\mu$m. (a) panel: curved beam path across the moving medium. (b) panel: intensity of the light beam at different depths in the medium. The optical parameters of the medium are the same as in fig.3; the vertical dashed lines correspond to the surfaces of the medium, whose thickness is taken as $L = 1.65\,\mu$m.

Figs.7-8, report the result of numerical calculations for the specific case of a moving EIT medium when the coupling beam is resonant ($\delta_c = 0$) and the probe beam is

[7] Even at the highest velocities here considered (v of the order of a few m/s), the use of the linearized form of the Lorentz transformations (3-5) is well justified: as the magnitude of the transverse Doppler effect of the probe and coupling beam $|\Delta\omega_\perp| \simeq \omega_0 v^2/c^2 \lesssim 10^{-8}\,\gamma_e$ the contribution of the terms in v^2 arising from the relativistic γ factor is negligible as compared to the one coming from the dispersion of ϵ.

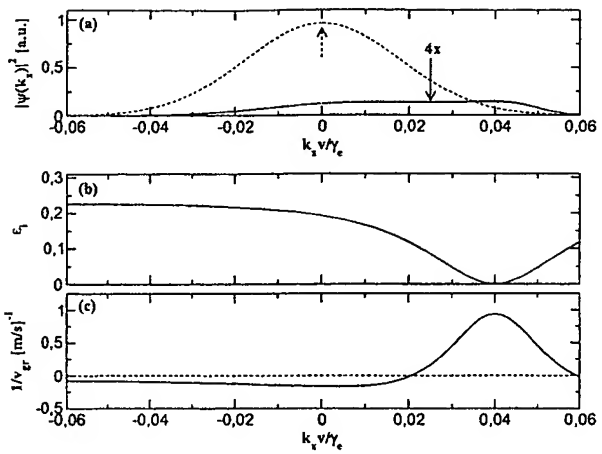

FIG. 8: Physical interpretation of the non-rectilinear light propagation of fig.7. (a) panel: spatial Fourier transform of the incident (dashed) and transmitted (solid) beam profile; for each spectrum, the arrow indicates the position of the spectral center of mass. For the sake of clarity, the transmitted spectrum has been multiplied by 4. (b) and (c) panels: absorption and inverse group velocity $1/v_{gr}$ spectra as a function of the transverse wavevector k_x. The corresponding Doppler-shifted frequency in the rest frame Σ' is $\omega' = \omega_0 - k_x v$. Since $\omega_0 - \omega_e = 0.04\,\gamma_e$, the resonance is found at $k_x v = 0.04\,\gamma_e$.

slightly detuned towards the blue ($\omega_0 - \omega_e = 0.04\,\gamma_e$). As one can verify by comparing the spectrum in fig.8a with the group velocity spectrum in fig.8c, most of the incident beam spectrum lies in the negative group velocity region ($k_x v < 0.02\,\gamma_e$), so the beam is initially dragged in the upstream direction. As absorption is weaker for the $k_x > 0$ components for which the Doppler-shifted frequency $\omega' = \omega_0 - k_x v$ is closer to resonance ($\partial \mathrm{Im}[k_z^{(in)}]/\partial k_x < 0$, see fig.8b), the negative $k_x < 0$ components are more rapidly quenched than the positive $k_x > 0$ components and the center of mass $k_x^{(cm)}$ of the spectral distribution moves towards the positive $k_x > 0$ values. As one can see in fig.8c, $\frac{\partial}{\partial k_x}\frac{1}{v'_{gr}} > 0$ in the region $0 < k_x v < 0.04\,\gamma_e$ of interest and therefore the curvature of the beam will be towards the downstream direction. After the first 1 μm of propagation, most of the k_x spectrum is found in the positive v'_{gr} region ($k_x v > 0.02\,\gamma_e$), so that the transverse Fresnel-Fizeau drag is from now on in the downstream direction (fig.7a).

As a consequence of the shift of the spectral center of mass k_x^{cm}, the beams exits from the rear face of the medium at a small but finite angle with respect to the normal towards the downstream direction. Although this effect is hardly visible on the scale of fig.8a, this small bending of the beam direction may have a significative effect on the subsequent rectilinear propagation of the beam in the free space.

Unfortunately, this effect of non-rectilinear propagation is associated to a rather severe absorption of the beam; for the specific case in figure, the transmitted intensity is of the order of 5% of the incident one (fig.7b).

It is also worth noticing that the curvature effect described in the present section follows from a reshaping of the beam in momentum space and hence is physically different from the ones discussed in [22, 23], which instead originate from a non-uniform velocity field of the slow-light medium.

B. Temporal and spatial coherence restoration

If both probe and coupling beams are exactly on resonance ($\omega_0 - \omega_e = \delta_c = 0$), both absorption $d\epsilon_i/d\omega'$ and group velocity $d^2\epsilon_r/d\omega'^2$ dispersion vanish, so that the effects described in sec.VI A do not take place. In the present subsection, we shall show how one can rather take advantage of the large value of $d^2\epsilon_i/d\omega'^2$ to improve the coherence level of a noisy incident probe beam. In sec.VI B 1, the case of *temporal* coherence restoration in a stationary EIT medium will be adressed, while in sec.VI B 2 we shall show how the same concepts can be applied in the case of a moving EIT medium to improve the level of *spatial* coherence.

1. *Temporal coherence restoration*

Consider an incident probe beam of carrier frequency ω_0 whose complex amplitude $E_0(t)$ is assumed as fluctuating in time over a characteristic time scale τ_c:

$$E(t) = E_0(t)\, e^{-i\omega_0 t}. \tag{37}$$

Following a standard model [48], the decay in time of the first-order coherence function $g^{(1)}(\tau)$ is taken to be Gaussian:

$$g^{(1)}(\tau) = \frac{\langle E_0^*(\tau)\, E_0(0)\rangle}{\langle E_0^*(0)\, E_0(0)\rangle} = \exp(-\tau^2/2\tau_c^2). \tag{38}$$

The frequency spectrum $|\tilde{E}(\omega)|^2$ of the beam, being proportional to the Fourier transform of the coherence function $g^{(1)}(\tau)$, is also Gaussian with linewidth $\sigma_c = 1/\tau_c$.

In a one-dimensional geometry, the propagation of a pulse through a stationary dielectric medium is described by the usual Fresnel equation:

$$k_z^2(\omega) = \epsilon(\omega)\,\frac{\omega^2}{c^2}. \tag{39}$$

In the neighborhood of the resonance at ω_e, the dielectric function of a slow light EIT medium can be approximately written as:

$$\epsilon(\omega) \simeq 1 + \frac{2c}{\omega_e v_{gr}}(\omega - \omega_e) + i\frac{\alpha}{2}(\omega - \omega_e)^2 \tag{40}$$

where v_{gr} is the group velocity at resonance and the real quantity α is given by:

$$\alpha = \left.\frac{d^2\epsilon_i(\omega)}{d\omega^2}\right|_{\omega=\omega_e} = \frac{4\pi f \gamma_e}{\Omega_c^4}. \tag{41}$$

At the lowest order in $\omega - \omega_e$, the real and imaginary parts of the wavevector $k_z(\omega)$ can then be written as:

$$k_z(\omega)|_r \simeq \frac{\omega_e}{c}\Big[1 + \frac{c}{\omega_e v_{gr}}(\omega - \omega_e)\Big]. \quad (42)$$

$$k_z(\omega)|_i \simeq \frac{\alpha\omega_e}{4c}(\omega - \omega_e)^2 \quad (43)$$

In particular, notice how the imaginary part of k_z is proportional to the square of $\omega - \omega_e$. Since after propagation over a distance L the amplitude of each frequency component is multiplied by a factor $\exp[ik_z(\omega)L]$, the frequency spectrum after propagation keeps its Gaussian shape, but the frequency linewidth is reduced to:

$$\sigma_c(L) = \frac{\sigma_c}{\sqrt{1 + \frac{\alpha\sigma_c^2\omega_e}{c}L}} \quad (44)$$

and the coherence time correspondingly increased to:

$$\tau_c(z) = \tau_c\sqrt{1 + \frac{\alpha\omega_e}{c\tau_c^2}L}. \quad (45)$$

Since the EIT medium does not provide amplification, a drawback of this filtering technique is that part of the incident intensity is lost during the line-narrowing process; the beam intensity after propagation through a distance L is in fact equal to:

$$I(L) = \frac{\sigma_c(L)}{\sigma_c(0)}I(0). \quad (46)$$

2. *Spatial coherence restoration*

For a moving EIT medium and a strictly monochromatic light beam at ω_0, a similar effect occurs in the k_x space. As discussed in full detail in sec.II, the propagation of light is described in this case by equation (7). For resonant probe and coupling beams, the imaginary part of $\mathrm{Im}[k_z^{(in)}]$ corresponding to absorption is proportional to $v^2k_x^2$:

$$\mathrm{Im}[k_z^{(in)}] \simeq \frac{\alpha\omega_0}{4c}v^2k_x^2. \quad (47)$$

As the amplitude of the transverse spatial fluctuations is proportional to the amplitude of non-vanishing k_x components, the spatial profile of the beam flattens as the beam propagates through the moving EIT medium. The faster the speed v of the medium, the more efficient the spatial coherence restoration process.

Results of a numerical calculation for a spatially noisy incident beam propagating through a moving EIT medium are presented in fig.9. Notice how the fluctuation amplitude is strongly suppressed during propagation. At the end of the process, the losses in the total intensity amount to 60%.

The overall shift of the beam which can be seen in the figure is due to the transverse Fresnel-Fizeau drag effect discussed in detail in sec.IV. Since both the probe and the coupling are resonant, the shift is directed in the downstream direction.

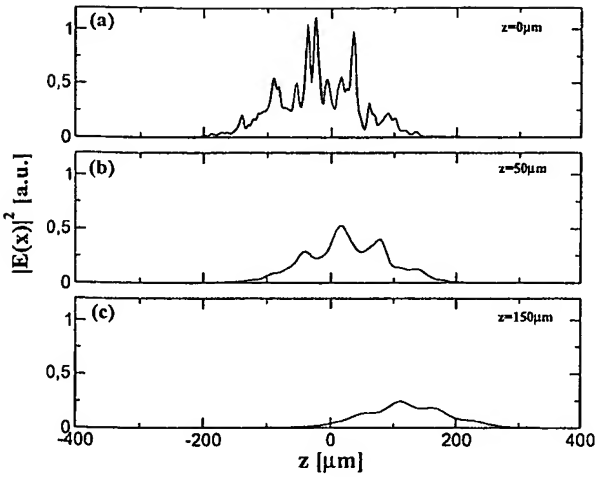

FIG. 9: Transverse spatial coherence restoration during propagation across a moving ($v = 1$ m/s) EIT medium in a fully resonant regime ($\delta_c = \omega_0 - \omega_e = 0$, $\omega_0 = \omega_e$). (a) panel: noisy incident beam profile. (b,c) panels: beam profile after propagation through the medium. Same medium parameters as in fig.3-7.

VII. CONCLUSIONS

In the present paper we have given a comprehensive analysis of the transverse Fresnel-Fizeau drag effect for light propagating across a uniform slab of moving EIT medium. All calculations have been performed using realistic parameters taken from EIT experiments with ultra-cold atomic clouds. Since our results are essentially a consequence of electromagnetically induced transparency, they are extremely general and thus hold through also for the recently prepared solid state EIT media. Depending on the detuning of the probe and coupling beams with respect to the medium resonance, different regimes have been identified.

In the presence of a slow and positive group velocity, the magnitude of the downstream Fresnel-Fizeau drag effect is predicted to be significantly enhanced with respect to previous experiments. In the regime of negative group velocity, an anomalous upstream Fresnel-Fizeau drag has been predicted to occur. Not only would this help in solving a long-standing controversy on the observability of such an effect, but it could also provide an interesting alternative way for experimentally detecting a negative group velocity.

For larger values of the velocity of the moving medium, higher order dispersion terms such as the dispersion of absorption and the dispersion of group velocity have been shown to play an important role in the phenomenology of light propagation. Depending on the specific choice of probe and coupling detuning, light propagation along curved paths can be observed, as well as the restoration of spatial coherence of a noisy beam.

The extension of the present analysis to more compli-

cated geometries including non-uniformly moving slow light media as well as probe pulses of finite duration will be the subject of future studies.

Acknowledgments

One of us (M.A.) should like to thank U. Leonhardt for enlightening discussions on the issue of slow light in moving media. Financial support from the EU (Contracts HPMF-CT-2000-00901 and HPRICT1999-00111), from the INFM (project PRA "photonmatter") and from the MIUR (grant PRIN 2002-028858) is greatly acknowledged. Laboratoire Kastler Brossel is a unité de Recherche de l'Ecole normale supérieure et de l'Université Pierre et Marie Curie, associée au CNRS.

[1] L. V. Hau, S. E. Harris, Z. Dutton, and C. H. Behroozi, Nature **397**, 594 (1999);
[2] S. Inouye *et al.*, Phys. Rev. Lett. **85**, 4225 (2000).
[3] M. M. Kash *et al.*, Phys. Rev. Lett. **82**, 5229 (1999);
[4] D. Budker , D. F. Kimball, S. M. Rochester, and V. V. Yashchuk, Phys. Rev. Lett. **83**, 1767 (1999).
[5] A. V. Turukhin *et al.*, Phys. Rev. Lett. **88**, 023602 (2002).
[6] M. S. Bigelow, N. N. Lepeshkin, and R. W. Boyd, Phys. Rev. Lett. **90**, 113903 (2003).
[7] O. Kocharovskaya, Y. Rostovtsev, and M. O. Scully, Phys. Rev. Lett. **86**, 628 (2001).
[8] D. F. Phillips *et al.*, Phys. Rev. Lett. **86**, 783 (2001);
[9] C. Liu, Z. Dutton, C. H. Behroozi, and L. V. Hau, Nature, **409**, 490, (2001).
[10] G. Alzetta, A. Gozzini, L. Moi, and G. Orriols, Nuovo Cimento **36B**, 5 (1976); E. Arimondo, G. Orriols, Lett. Nuovo Cimento **17**, 333 (1976).
[11] E. Arimondo in *Progress in Optics XXXV*, ed. by E. Wolf, Elsevier Science, (1996) pag.257.
[12] T.W. Hänsch, P.E. Toschek, Z. Phys. **236**, 213 (1970).
[13] S. Harris, Phys. Today **50**, No. 7, 36 (1997).
[14] A. B. Matsko *et al.*, Adv. At. Mol. Opt. Phys. **46**, 191 (2001).
[15] J. Marangos, J. Mod. Opt. **45**, 471 (1998).
[16] S. E. Harris, J. E. Field, and A. Kasapi, Phys. Rev. A **46**, R29 (1992);
[17] S. E. Harris and L. V. Hau, Phys. Rev. Lett. **82**, 4611, (1999);
[18] M. D. Lukin and A. Imamoglu, Phys. Rev. Lett. **84**, 1419 (2000).
[19] M. D. Lukin, S. F. Yelin, and M. Fleischhauer, Phys. Rev. Lett. **84**, 4232 (2000).
[20] M. Fleischhauer and M. D. Lukin, Phys. Rev. Lett. **84**, 5094 (2000).
[21] A. B. Matsko, Y. V. Rostovtsev, H. Z. Cummins, and M. O. Scully, Phys. Rev. Lett. **84**, 5752 (2000).
[22] U. Leonhardt and P. Piwnicki, Phys. Rev. Lett. **84**, 822 (2000);
[23] U. Leonhardt, Phys. Rev. A **62**, 012111 (2000);
[24] U. Leonhardt and P. Piwnicki, J. Mod. Opt. **48**, 977 (2001);
[25] U. Leonhardt, Phys. Rev. A **65**, 043818 (2002);
[26] U.Leonhardt, Nature **415**, 406 (2000);
[27] J. Fiurasek, U. Leonhardt and R. Parentani, Phys. Rev. A **65**, 011802 (2002);
[28] U. Leonhardt, Phys. Rev. A **62**, 012111 (2000). Physics World, **15**, No 2, 7, (2002)
[29] M. Artoni, G. C. La Rocca, F. S. Cataliotti, and F. Bassani, Phys. Rev. A **63**, 023805 (2001).
[30] M. Artoni, I. Carusotto, G. C. La Rocca, and F. Bassani, Phys. Rev. Lett. **86**, 2549 (2001).
[31] R. V. Jones, Proc. Roy. Soc. London A **328**, 337 (1972).
[32] R. V. Jones, Proc. Roy. Soc. London A **345**, 351 (1975).
[33] H. C. Ko and C. W. Chuang, Astroph. Journ. **222**, 1012 (1978); H. C. Ko, Astroph. Journ. **231**, 589 (1979).
[34] I. Lerche, Astroph. Journ. **187**, 589 (1974).
[35] J. D. Jackson, *Classical Electrodynamics* (J. Wiley, New York, 1975).
[36] M. A. Player, Proc. Roy. Soc. London A **345**, 343 (1972).
[37] G. L. Rogers, Proc. Roy. Soc. London A **345**, 345 (1972).
[38] M. Artoni, I. Carusotto, G. C. La Rocca, and F. Bassani, J. Opt. B **4**, S345 (2002).
[39] L. D. Landau and E. M. Lifshitz, *Electrodynamics of continuous media*, Pergamon Press, London, 1960.
[40] S. Chu and S. Wong, Phys. Rev. Lett. **48**, 738 (1982);
[41] A. M. Steinberg, P. G. Kwiat, and R. Y. Chiao, Phys. Rev. Lett. **71**, 701 (1993);
[42] Ph. Balcou and L. Dutriaux, Phys. Rev. Lett. **78**, 851 (1997).
[43] L. J. Wang, A. Kuzmich, and A. Dogariu, Nature **406**, 277 (2000).
[44] V.G.Veselago, Sov. Phys. Usp. **10**, 509 (1968); D.R.Smith, *et al.*, Phys. Rev. Lett. **84**, 4184 (2000)
[45] P. W. Milonni, J. Phys. B: At. Mol. Opt. Phys. **35**, R31 (2002).
[46] M. Artoni and R.Loudon, Phys. Rev. A **55**, 1347 (1997).
[47] L. Muschietti and C. T. Dum, Phys. Fluids B **5**, 1383 (1993).
[48] R. Loudon, *The quantum theory of light*, Clarendon Press, Oxford, 1973.